2011-03-17

Evaluation of Portable Devices for Monitoring Microcracking of Cement-Treated Base Layers

Charles A. Hope
Brigham Young University - Provo

Evaluation of Portable Devices for Monitoring Microcracking of Cement-Treated Base Layers

Charles A. Hope

A thesis submitted to the faculty of
Brigham Young University
in partial fulfillment of the requirements for the degree of

Master of Science

W. Spencer Guthrie, Chair
A. Woodruff Miller
Travis M. Gerber

Department of Civil and Environmental Engineering

Brigham Young University

April 2011

ABSTRACT

Evaluation of Portable Devices for Monitoring Microcracking
of Cement-Treated Base Layers

Charles A. Hope
Department of Civil and Environmental Engineering, BYU
Master of Science

A relatively new method used to reduce the amount of cement-treated base (CTB) shrinkage cracking is microcracking of the CTB shortly after construction. Three portable instruments used in this study for monitoring the microcracking process include the heavy Clegg impact soil tester (CIST), portable falling-weight deflectometer (PFWD), and soil stiffness gauge (SSG). The specific objectives of this research were 1) to evaluate the sensitivity of each of the three portable instruments to microcracking, and 2) to compare measurements of CTB stiffness reduction obtained using the three devices.

The test locations included in this study were Redwood Drive and Dale Avenue in Salt Lake City, Utah; 300 South in Spanish Fork, Utah; and a private access road in Wyoming. Experimental testing in the field consisted of randomized stationing at each site; sampling the CTB immediately after the cement was mixed into the reclaimed base material; compacting specimens for laboratory testing; and testing the CTB immediately after construction, immediately before microcracking, immediately after each pass of the vibratory roller during the microcracking process, and, in some instances, three days after microcracking.

Several linear regression analyses were performed after data were collected using the CIST, PFWD, and SSG during the microcracking process to meet the objectives of this research. Results from the statistical analyses designed to evaluate the sensitivity of each of the three portable instruments to microcracking indicate that the PFWD and SSG are sensitive to microcracking, while the CIST is insensitive to microcracking. Results from the statistical analyses designed to compare measurements of CTB stiffness reduction demonstrate that neither of the instrument correlations involving the CIST are statistically significant. Only the correlation between the PFWD and SSG was shown to be statistically significant.

Given the results of this research, engineers and contractors should utilize the PFWD or SSG for monitoring microcracking of CTB layers. The heavy CIST is unsuitable for monitoring microcracking and should not be used. For deriving target CTB stiffness reductions measured using either the PFWD or SSG from specified targets measured using the other, engineers and contractors should utilize the correlation chart developed in this research.

Key words: cement-treated base, cement slurry, Clegg impact soil tester, full-depth reclamation, microcracking, portable falling-weight deflectometer, reclaimed asphalt pavement, soil stiffness gauge, stabilization

ACKNOWLEDGEMENTS

I wish to express my sincere gratitude to Dr. W. Spencer Guthrie for his assistance, encouragement, and enthusiasm during the span of this research and throughout my time in the Materials and Pavements Research Group. Great appreciation is felt for the resources provided by the Portland Cement Association and the Brigham Young University Department of Civil and Environmental Engineering. I would like to acknowledge research team members Mark Butler, Paul Dixon, Jeremy Dye, Jeff Hoki, Adam Homewood, Tyler Quick, Maile Rogers, Tyler Rogers, Scott Shea, Chase Thomas, and Bryan Wilson for assisting with data collection and compilation. I am grateful for my family's unwavering love and continuous motivation during the course of my academic career. I wish to give thanks to the Clayton family for their dedicated support and uplifting words of encouragement. Finally, I would like to express deep appreciation to my wonderful wife, Emily Hope, for her untiring love and support throughout all my activities. Emily, je t'aime très très très fort.

TABLE OF CONTENTS

LIST OF TABLES

LIST OF FIGURES

1 INTRODUCTION

1.1 Problem Statement

As the roadway system in the United States continues to age, engineers must focus greater attention on identifying effective solutions for maintenance, rehabilitation, and reconstruction of pavements. Concerning reconstruction, one current and sustainable practice is the recycling of existing pavement materials. Through the process of full-depth reclamation (FDR), aged asphalt layers are pulverized and mixed with the underlying base material, and a stabilizer such as portland cement can be added to create a cement-treated base (CTB).

CTB is commonly specified in pavement construction for all classes of roadways, from interstate highways to local streets. CTB material is an intimate mixture of aggregate and portland cement that is tightly compacted to form a strong, durable pavement material (Portland Cement Association 2006). The addition of cement increases the strength and stiffness of the treated material and therefore offers greater structural support to the surface layer and greater protection of the underlying subgrade. Cement can be used to improve a variety of materials because of its ability to stabilize clays, sands, silts, and gravels (American Concrete Institute 1990). In addition, cement-stabilized soils and aggregates provide excellent load transfer, offer increased resistance to rutting, are practically impervious, are minimally affected by moisture, resist cyclic freeze-thaw damage, prevent migration of fines, are non-erodible, and continue gaining strength with age (George 2002, Portland Cement Association 2006). However, due to

the shrinkage that occurs as portland cement hydrates, CTB layers are susceptible to cracking. When the CTB layer is surfaced with asphalt, shrinkage cracks can propagate upwards and cause distresses in the form of transverse and/or block cracking.

The occurrence of shrinkage cracking is influenced by both CTB material properties and construction practices. Regarding material properties, previous research has demonstrated that shrinkage cracks are influenced by cement content, moisture content, ambient weather conditions, aggregate properties, type and time of surfacing, and self-desiccation of hydrating cement (Scullion 2002). Regarding construction practices, shrinkage cracking can be reduced by improving mixing quality, ensuring uniform distribution of cement consistent with project specifications, adding soil admixtures such as fly ash, compacting the cement-treated material at or slightly less than optimum moisture content (OMC), moist curing immediately after final compaction, and utilizing a relatively new procedure called microcracking, or pre-cracking (George 2002, Portland Cement Association 2003, Scullion 2002).

Of particular interest to this research, microcracking involves passing a vibratory roller over a newly constructed CTB in order to relieve the internal shrinkage stresses that develop during the initial cement hydration. The desired result of microcracking is a network of fine, closely spaced cracks that are uniformly distributed throughout the CTB. The findings of other researchers indicate that microcracking is adequate when the CTB layer experiences a 50 to 70 percent reduction in stiffness, as measured with a falling-weight deflectometer (FWD), compared to the baseline measurement (Sebesta and Scullion 2004). Because the number of vibratory roller passes required to achieve this level of stiffness reduction is typically dependent on project-specific material properties and construction practices, a means of monitoring CTB stiffness in the field is generally required to ensure that microcracking is performed properly.

Strength reductions in CTB during microcracking have commonly been monitored using a FWD (Sebesta and Scullion 2004). The FWD is a trailer- or truck-mounted device that is comparatively expensive to purchase and maintain. While some state departments of transportation (DOTs) own FWDs, most local agencies do not have ready access to this testing equipment. Consequently, investigation of the potential use of other instruments for monitoring microcracking is needed. In this research, the heavy Clegg impact soil tester (CIST), portable falling-weight deflectometer (PFWD), and soil stiffness gauge (SSG) were specifically identified as possible alternative tools for monitoring microcracking. Not only are all three devices much less expensive than a FWD, they are also portable, meaning that they can be easily carried by an operator from place to place on a construction site without the use of a vehicle. While some information is available in the literature on the use of these devices for monitoring microcracking (Goehl et al. 2006, Scullion 2002, Scullion et al. 2005, Sebesta 2005a, Sebesta 2005b, Sebesta 2006, Sebesta and Scullion 2004), the sensitivity of each instrument to the progression of microcracking has not been formally evaluated, nor have these different measurements of CTB stiffness reduction during microcracking been compared. The authors of those studies instead focused on evaluating CTB strength loss and recovery after microcracking, in addition to assessing the immediate and long-term effects of microcracking on the pavement structure.

Comparative data on the utility of the CIST, PFWD, and SSG for monitoring microcracking would be beneficial to practitioners who desire to use microcracking as a technique for reducing shrinkage cracking in CTB but who do not have access to a FWD. Therefore, the specific objectives of this research were 1) to evaluate the sensitivity of each of the three portable instruments to microcracking, and 2) to compare measurements of CTB stiffness reduction obtained using the three devices.

1.2 Scope

The research conducted in this study involved monitoring the CTB microcracking process using the CIST, PFWD, and SSG on four different roads in Utah and Wyoming. These reconstruction projects utilized FDR with cement stabilization. Cement was distributed in slurry form at the Utah projects and in powder form at the Wyoming project. Specified cement contents were all 4 percent by dry weight of aggregate, and the CTB layers ranged in thickness from 6 to 9 in. Field testing was supplemented by laboratory material characterizations on each project.

1.3 Outline of Report

This report contains five chapters. Chapter 1 includes the problem statement and scope of this research. Chapter 2 presents background information on microcracking of CTB and describes instruments potentially useful for monitoring microcracking. Chapter 3 describes the experimental plan, field and laboratory testing procedures, and statistical analyses. Chapter 4 reports the results of testing and analysis and provides a discussion of the research findings. Chapter 5 gives a summary of the research, highlights important research findings, and offers recommendations.

2 BACKGROUND

2.1 Overview

The following sections present the findings of a literature review focused on the use of cement stabilization, the application of microcracking to reduce shrinkage cracking, and instruments potentially useful for monitoring microcracking.

2.2 Use of Cement Stabilization

Portland cement has been used in soil stabilization since 1915 (American Concrete Institute 1990) because of its strengthening properties when mixed with base material. CTB is similar to concrete in that the aggregates within the material are bonded together during the cement hydration process when calcium silicates react with water to produce the cementitious product calcium silicate hydrate (Mindess et al. 2003). Unlike concrete, however, only a fraction of the soil and aggregate particles in soil-cement are coated with cement (American Concrete Institute 1990).

Cement can be used on a variety of materials because of its ability to stabilize fines, such as clays and silts, as well as coarse aggregates, such as gravels, sands, and pulverized asphalt (American Concrete Institute 1990). Cement stabilization used in conjunction with FDR reduces material transportation costs, conserves decreasing supplies of virgin aggregates, and causes minimal impact to the traveling public (Prusinski 2000). In addition, cement-stabilized soils

provide excellent load transfer, are minimally affected by moisture, are more uniform than unstabilized base, and continue gaining strength with age even under traffic, therefore increasing the capacity and durability of the pavement (Adaska and Luhr 2004, Prusinski 2000). These properties are especially desirable for flexible pavements (George 2002, Portland Cement Association 2006).

Cement can be added in two ways: cement powder or cement slurry. Cement powder is spread directly from a cement spreader truck, but the resulting fugitive cement dust can produce unacceptable air quality as shown in Figure 2-1. Cement slurry can be distributed directly out of the chute of a mixer truck as illustrated in Figure 2-2, or a portable slurry spreader may be attached to the chute for more uniform cement distribution as shown in Figure 2-3 (Hope et al. 2004).

Figure 2-1: Cement powder application.

Figure 2-2: Cement slurry application directly from a truck chute.

Figure 2-3: Cement slurry application using a cement slurry spreader.

2.3 Application of Microcracking

Although CTB provides excellent support to the surface course, CTB experiences shrinkage cracking that can lead to premature pavement damage. Shrinkage is a natural

characteristic of soil-cement and is not considered to be structural failure (Norling 1973). Shrinkage cracks are fractures or fissures that are found in the CTB matrix and are caused by both internal and external stresses on the base layer. Variations in temperature and hydration of the cement are example sources of internal stress. Traffic loads and subgrade expansion or shrinkage are example sources of external stress. A CTB will crack when the tensile strength of the base is exceeded by the applied stress acting on the base (George 1973, Hajek 1972).

Shrinkage cracks in CTB comprising flexible pavement structures often propagate upward into the asphalt surface layer. While small reflective cracks are aesthetically displeasing, they have relatively little effect on the serviceability of the pavement (George 1973, George 2002, Adaska and Luhr 2004).

Though small reflective cracks do not present performance issues, cracks greater than 0.25 in. in width can result in poor load transfer and greatly reduce the service life of roads (Adaska and Luhr 2004). Reflective cracks can cause non-uniform stress distributions in pavement structures under traffic loading and can lead to other types of pavement failures, including fatigue cracking (Pretorius et al. 1972). In addition, water infiltration is more common where reflective cracks are found; the presence of water causes the base and the subgrade layers to be more susceptible to structural failures induced by erosion and deterioration under freeze-thaw cycling (Crane et al. 2006).

Several agencies have invested considerable effort and funds to find solutions to the CTB shrinkage cracking problem. Some have investigated the possibilities of altering the soil properties or using cement additives to change the properties of soil-cements (Adaska and Luhr 2004, Scullion et al. 2005, Wang 1973). A relatively new method used to reduce the amount of CTB shrinkage cracking is microcracking of the CTB shortly after construction (Goehl et al.

2006, Litzka and Haslehner 1995, Prusinski 2000, Scullion 2002, Sebesta 2006, Sebesta and Scullion 2002). This process reduces the severity of shrinkage cracking by creating a network of fine cracks within the CTB that relieve initial shrinkage stresses (Goehl et al. 2006). In other research, the introduction of these fine cracks has been shown to be accompanied by an immediate but temporary decrease in CTB strength; with continued curing, a nearly full recovery in CTB strength occurs in subsequent days due to the autogenous healing properties of soil-cement (Sebesta and Scullion 2004, Halsted 2006).

The microcracking method involves the application of a vibratory roller to a CTB layer only 2 to 3 days after compaction, as shown in Figure 2-4, to reduce the stiffness of the CTB layer by a target value of 50 to 70 percent as measured using a FWD. The vibratory roller employed for microcracking should be the same or equivalent to the roller used for original compaction of the CTB and should generally be operated at 2 to 3 mph, with vibration at maximum amplitude (Sebesta 2006). Depending on project conditions, the speed of the vibratory roller may need to be adjusted to ensure that the CTB is properly microcracked.

Before and during microcracking, the CTB modulus is measured to determine when the target reduction in strength has been achieved. As many as six passes, where a pass is defined as a single coverage, may be required on a given project. In addition to taking measurements of the base stiffness using instruments, inspectors may evaluate microcracking visually. The process of microcracking should not significantly change the texture of the surface. In fact, cracks should be fine enough to be barely noticeable. Microcracked surfaces should not experience raveling or spalling. To ensure continued CTB curing after microcracking, the layer should be frequently watered, as shown in Figure 2-5, or an impermeable curing membrane should be applied (Sebesta 2005b).

Figure 2-4: Microcracking using a vibratory roller.

Figure 2-5: Moist curing using a water truck.

2.4 Instruments for Monitoring Microcracking

Beyond the FWD, the CIST, PFWD, and SSG are available for measuring the stiffness of soil and aggregate layers (Guthrie et al. 2005). All of these instruments have been utilized to

characterize the in-situ properties of CTB and were evaluated in this research as tools for monitoring the microcracking process. Each instrument is described in the following sections.

2.4.1 Clegg Impact Soil Tester

The CIST is a relatively simple instrument comprised of a slide hammer, a guide tube, and an electronic digital readout. Several models of the CIST are available, each with a different hammer weight. Figure 2-6 shows the 44-lb heavy CIST utilized in this research. The diameter of the slide hammer on this instrument is 5 in.

A CIST test is performed by dropping the slide hammer four times at the desired test point. The deceleration of the slide hammer upon impact with the soil is measured by an

Figure 2-6: CIST testing.

accelerometer mounted on top of the hammer, which is connected to a digital readout device. The peak deceleration of the hammer is reported as a Clegg impact value (CIV), where one CIV unit is equal to 10 gravities, or 10 times the acceleration of gravity (Clegg Instruction Manual 1993).

According to the Clegg instruction manual, the CIV scale ranges from 0 to 199.9 in tenths increments. CIV values may be correlated to California bearing ratio (CBR) and to resilient modulus using empirically derived relationships among these properties (Thompson 2009). CIV values are also used to determine the Clegg hammer elastic modulus of soil and aggregate layers. Only the CIV is used in this report.

2.4.2 Portable Falling-Weight Deflectometer

The PFWD is an instrument comprised of a slide-hammer assembly, a loading plate, and deflection sensors. The PFWD is equipped with a physical or wireless connection that enables the operator to connect a personal digital assistant (PDA) to the instrument and immediately retrieve data from the PFWD. The readings displayed on the PDA include the composite modulus and the deflection measured by each sensor. A picture of the PFWD used in this research is provided in Figure 2-7.

The PFWD is operated by placing the loading plate on the pavement surface and positioning the external sensors at specified radial distances from the center of the loading plate; in this research, three sensors spaced at 0, 12, and 24 in. were used with a 7.9-in.-diameter plate. The steel sliding weight is then dropped from a specified height. The sizes of the available loading plates, the mass of the falling weight, and the height from which the falling weight is dropped depend on the PFWD model used. As the sliding weight impacts the loading plate,

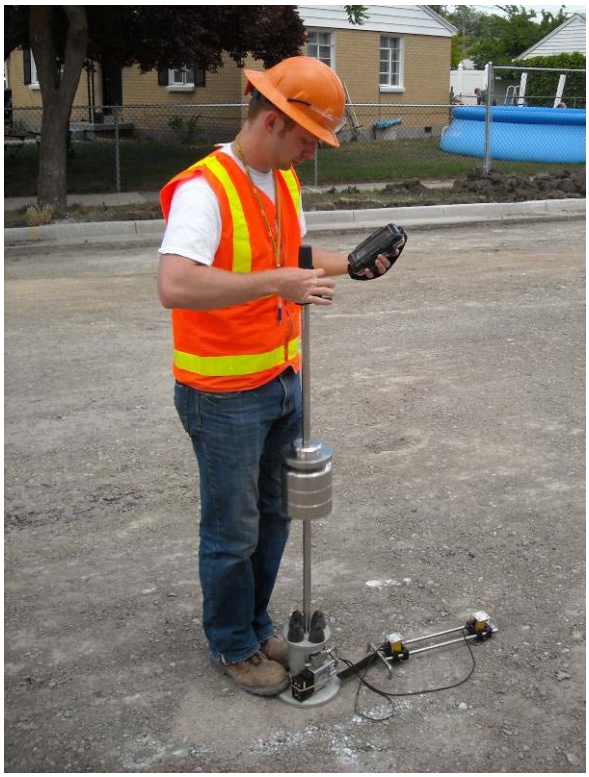

Figure 2-7: PFWD testing.

which is typically protected with neoprene pads, the ground deflects, and the displacements are measured using accelerometers or velocity transducers. The force from the falling weight is measured by an internal load cell.

In concept, the PFWD is similar to the FWD but has a lower loading capacity and fewer sensors. In addition, the PFWD is much lighter and less expensive than the FWD. Similar to FWD data analyses, data collected using the PFWD can be processed using computer software to determine the modulus of each pavement layer or to determine a composite modulus of the full pavement structure. Modulus values have units of force per area. Only the composite modulus was used in this research.

2.4.3 Soil Stiffness Gauge

Depicted in Figure 2-8, the SSG is a compact cylindrical device, weighing 22 lbs, with a ring-shaped bottom foot having an outside diameter of 4 in. A rigid column connects an internal force sensor and a shaker located at the center of the instrument; the shaker drives the sensors located in the foot that measure force and displacement. The SSG imparts small displacements to the soil, less than 0.00005 in., at 25 steady-state frequencies between 100 and 196 Hz (Humboldt 2002). The corresponding stress and displacement data are then used to compute the soil stiffness.

The SSG is operated by positioning the foot on a thin bed of fine soil or moist sand to ensure that at least 60 percent of the foot is in direct contact with the soil. Pressing a button on the top of the instrument starts a test, which requires about 60 seconds. The test results are

Figure 2-8: SSG testing.

shown in the digital display on the top of the SSG. Along with the stiffness value, the associated signal-to-noise ratio, which reflects the ambient vibrations in the ground, and the standard deviation, which captures measurement variability, are displayed. The SSG calculates stiffness as shown in Equation 2-1 (Humboldt 2002):

$$S = \frac{P}{\delta} \tag{2-1}$$

where S = stiffness (MN/m)

P = force (MN)

δ = displacement of the soil (m)

2.5 Summary

Cement stabilization used in conjunction with FDR reduces material transportation costs, conserves decreasing supplies of virgin aggregates, and causes minimal impact to the traveling public. Although CTB provides excellent support to the surface course, CTB experiences shrinkage cracking that can lead to premature pavement damage. Shrinkage cracks in CTB comprising flexible pavement structures often propagate upward into the asphalt surface layer. Reflective cracks can cause non-uniform stress distributions in pavement structures under traffic loading and can lead to other types of pavement failures, including fatigue cracking. A relatively new method used to reduce the amount of CTB shrinkage cracking is microcracking of the CTB shortly after construction. This process reduces the severity of shrinkage cracking by creating a network of fine cracks within the CTB that relieve initial shrinkage stresses. Three portable instruments that have been used for monitoring the microcracking process include the CIST, PFWD and SSG.

3 EXPERIMENTAL PROCEDURES

3.1 Overview

This research focused on evaluating the sensitivity of the CIST, PFWD, and SSG to microcracking of CTB layers and comparing measurements of CTB stiffness reduction obtained using the three devices. The test locations included in this study were Redwood Drive in Salt Lake City, Utah; Dale Avenue in Salt Lake City, Utah; 300 South in Spanish Fork, Utah; and a private access road 30 miles east of Rock Springs, Wyoming. Testing during reconstruction at Redwood Drive, Dale Avenue, Spanish Fork, and Wyoming was conducted during August 2008, June 2009, August 2009, and August 2009, respectively.

Prior to reconstruction, these four pavements consisted of untreated base course material with asphalt surfacing. The specifications for each project required FDR with cement stabilization, with slurry required for the Utah projects and powder required for the Wyoming project.

The following sections document the field and laboratory testing procedures, as well as the methods used for data analysis. In all tables throughout this chapter, the presence of a hyphen indicates that the data entry was not applicable.

3.2 Field Testing

As described in the following sections, experimental testing in the field consisted of randomized stationing at each site; sampling the CTB immediately after the cement was mixed into the reclaimed base material; compacting specimens for laboratory testing; and testing the CTB immediately after construction, immediately before microcracking, immediately after each pass of the vibratory roller during the microcracking process, and, in some instances, three days after microcracking.

3.2.1 Station Layout

Each test site varied in length. Redwood Drive was 1537 ft, Dale Avenue was 320 ft, Spanish Fork was 408 ft, and the Wyoming access road was divided into six sites, referred to as A through F, that were 2000 ft each. Redwood Drive, Dale Avenue, Spanish Fork, and the six Wyoming sites were 38, 38, 66, and 30 ft wide, respectively.

Ten testing stations were chosen at each site using random sampling techniques, where every possible testing station within a given site had an equal chance of being selected. The random factors utilized at all sites for selecting longitudinal station positions are presented in Table 3-1; in each case, each random factor was multiplied by the total length of each site to compute the station location. At the Redwood Drive, Dale Avenue, and Spanish Fork sites, the transverse station positioning was strategically determined by alternating from one lane to the other while avoiding the wheel paths of the mixer trucks; the transverse stations were necessarily positioned out of the wheel paths to facilitate cement sampling during the slurry application. At the Wyoming sites, where slurry was not distributed and cement content was not measured, transverse station locations were determined relative to the edge of the road using the random

factors listed in Table 3-2. Tables 3-3 to 3-7 give the location of each station at the Redwood Drive, Dale Avenue, Spanish Fork, and Wyoming sites, respectively. All of the sampling and testing conducted in this research were performed at the same stations at each site, unless otherwise indicated.

The station layouts for the test sites are displayed graphically in Figures 3-1 to 3-4. The layout of all the Wyoming sites was the same as that shown in Figure 3-4 for Wyoming A. The relative locations of the Wyoming sites to each other are depicted in Figure 3-5.

Table 3-1: Random Factors Used to Determine Longitudinal Station Locations

Station	Random factor
1	0.02
2	0.07
3	0.12
4	0.18
5	0.26
6	0.35
7	0.43
8	0.67
9	0.81
10	0.87

Table 3-2: Random Factors Used to Determine Transverse Station Locations for Wyoming Sites

Station	Random factor
1	0.24
2	0.64
3	0.97
4	0.29
5	0.91
6	0.53
7	0.66
8	0.54
9	0.32
10	0.87

Table 3-3: Station Layout for Redwood Drive

Station	Distance from north end (ft)	Distance from east curb (ft)
North End	0.0	-
1	30.7	8.0
2	111.6	28.0
3	184.4	8.0
4	276.7	22.0
5	399.6	8.0
6	538.0	28.0
7	660.9	8.0
8	1029.8	18.0
9	1245.0	8.0
10	1337.2	28.0
South End	1537.0	-

Table 3-4: Station Layout for Dale Avenue

Station	Distance from west end (ft)	Distance from south curb (ft)
West End	0.0	-
1	6.4	5.0
2	22.4	28.0
3	38.4	6.0
4	57.6	22.0
5	83.2	6.0
6	112.0	28.0
7	137.6	6.0
8	214.4	18.0
9	259.2	6.0
10	278.4	28.0
East End	320.0	-

Table 3-5: Station Layout for Spanish Fork

Station	Distance from east end (ft)	Distance from south curb (ft)
East End	0.0	-
1	8.2	16.0
2	28.6	50.0
3	49.0	8.0
4	73.4	34.0
5	106.1	16.0
6	142.8	50.0
7	175.4	8.0
8	273.4	34.0
9	330.5	16.0
10	355.0	50.0
West End	408.0	-

Table 3-6: Station Layout for Wyoming A through D

Station	Distance from north end (ft)	Distance from east edge (ft)
North End	0.0	-
1	40.0	3.6
2	140.0	9.6
3	240.0	14.6
4	360.0	4.4
5	520.0	13.7
6	700.0	8.0
7	860.0	9.9
8	1340.0	8.1
9	1620.0	4.8
10	1740.0	13.1
South End	2000.0	-

Table 3-7: Station Layout for Wyoming E and F

Station	Distance from north end (ft)	Distance from west edge (ft)
North End	0.0	-
1	40.0	3.6
2	140.0	9.6
3	240.0	14.6
4	360.0	4.4
5	520.0	13.7
6	700.0	8.0
7	860.0	9.9
8	1340.0	8.1
9	1620.0	4.8
10	1740.0	13.1
South End	2000.0	-

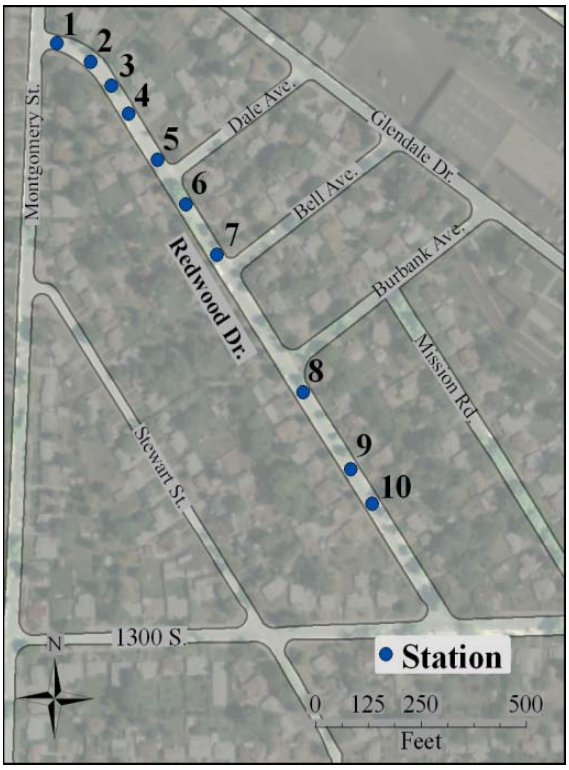

Figure 3-1: Station layout for Redwood Drive.

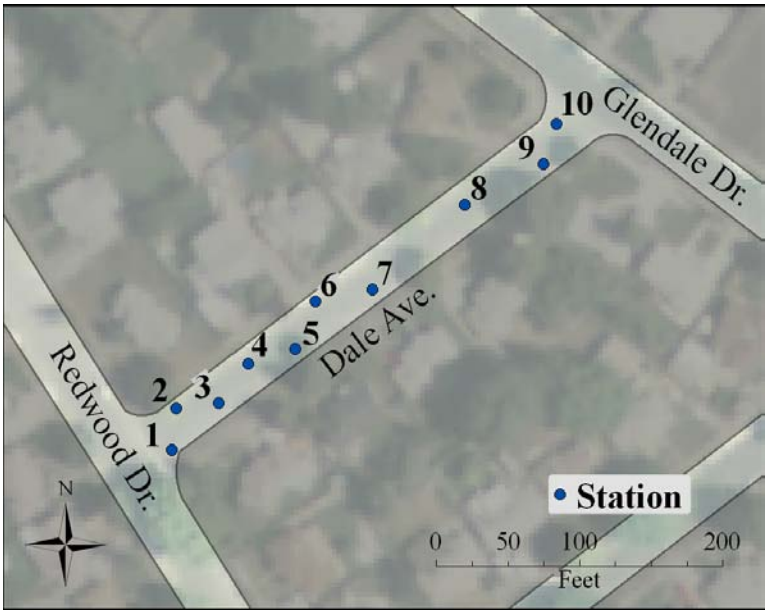

Figure 3-2: Station layout for Dale Avenue.

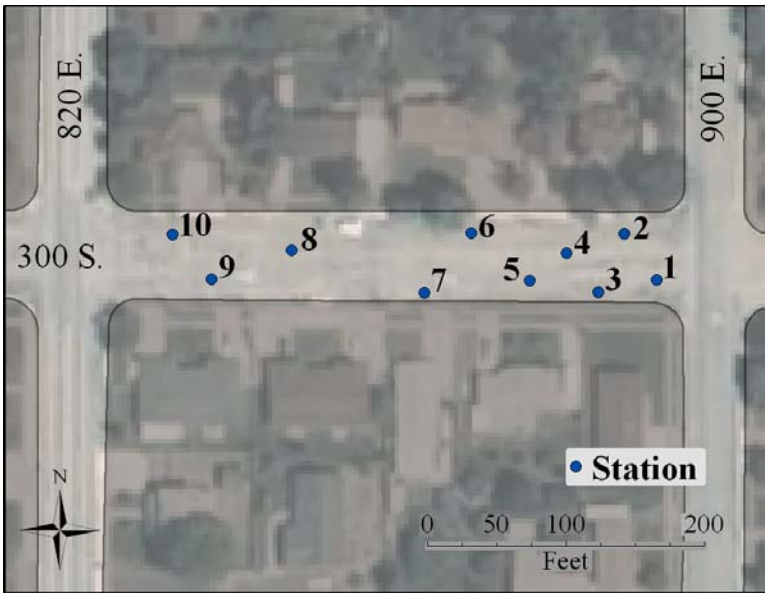

Figure 3-3: Station layout for Spanish Fork.

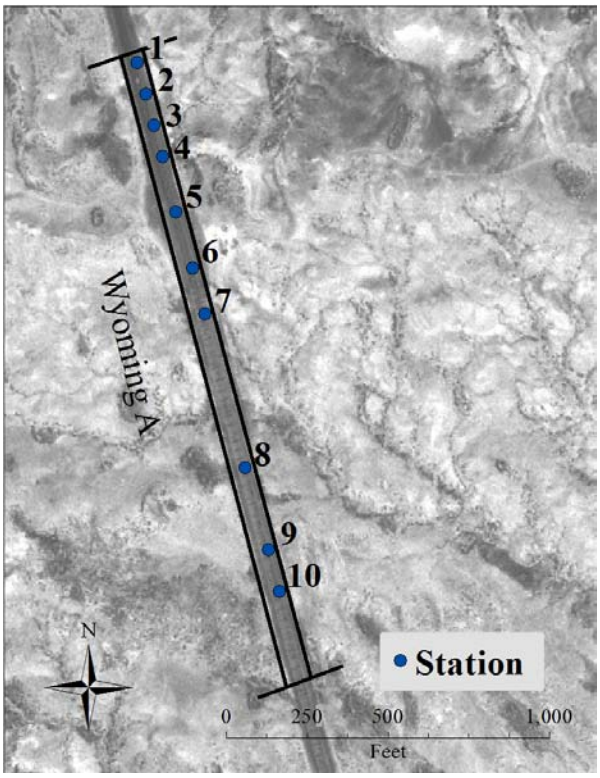

Figure 3-4: Station layout for Wyoming A.

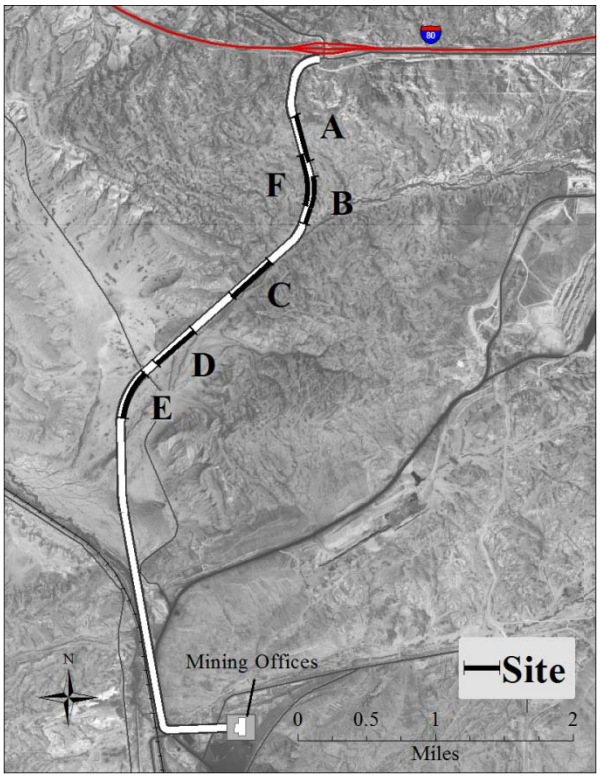

Figure 3-5: Site layout for Wyoming A through F.

3.2.2 Sampling Procedures

Properties of the original base and subgrade were obtained by testing those layers using a dynamic cone penetrometer (DCP) and by sampling the existing material for laboratory testing. DCP tests were performed before the surface course was pulverized and mixed into the base material. As displayed in Figure 3-6, a DCP consists of a metal rod with a standard cone tip that is driven into the ground by a manually operated slide hammer; the measured DCP penetration rates were used to determine CBRs for both the base and subgrade layers at the time of testing following Equation 3-1 (Webster et al. 1992):

Figure 3-6: DCP testing.

$$CBR = \frac{292}{PR^{1.12}} \tag{3-1}$$

where CBR = California bearing ratio (%)

PR = Penetration rate (mm/blow)

One neat asphalt sample of the original asphalt surface course was collected from each site, except Spanish Fork, for determining asphalt content in the laboratory. Samples of the reclaimed base material were then obtained from each station immediately before the application of cement at each site. The samples of reclaimed asphalt pavement (RAP)-base blend were placed in plastic bags as depicted in Figure 3-7 and transported to the Brigham Young University (BYU) Highway Materials Laboratory for material characterization testing.

Figure 3-7: Sampling of RAP-base blend.

Cement slurry samples were also collected on sites where cement slurry was applied. At the Redwood Drive, Dale Avenue and Spanish Fork sites, 2.5-in.-deep pans having a length of 17 in. and a width of 12.5 in. were placed on the graded RAP-base blend prior to the introduction of cement in order to measure the amount of cement slurry applied at each station, as illustrated in Figure 3-8. The pans were weighed before and after the application of cement slurry. At the Wyoming sites, the cement was spread as cement powder, and no in-situ cement content was measured. The design cement content for all testing locations was 4 percent by weight of dry aggregate.

At Redwood Drive, the cement slurry was distributed onto the RAP-base blend directly from the chute of a mixer truck, as shown in Figure 2-2, and the cement was subsequently mixed into the base material to a depth of 8 in. using a reclaimer. At Dale Avenue and Spanish Fork, the cement slurry was distributed onto the RAP-base blend using a slurry spreader that attached directly onto the chute of the cement truck as displayed in Figure 2-3. The nozzles on the

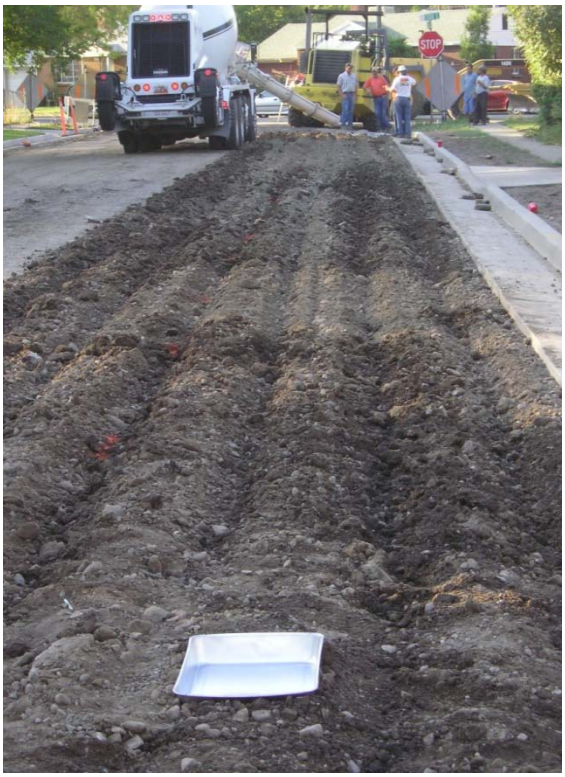

Figure 3-8: Collecting cement slurry.

spreader were adjusted as needed to compensate for differences in hydraulic head from one end of the spreader to the other due to cross-slopes on the roadways. The cement was mixed into the base material to a depth of 8 in. using a reclaimer. At the Wyoming sites, cement powder was applied using a pneumatic distributor truck as shown in Figure 2-1. The cement powder was subsequently mixed into the base material to a depth of 9 in. using a reclaimer. A water truck connected to the reclaimer supplied the water necessary to bring the base material to OMC.

Immediately after the cement was mixed into the road base at a given station, two plastic bags were filled with CTB material, which was then immediately used to make three to four specimens of 4.0-in. diameter and approximately 4.6-in. height. The specimens were compacted with manually operated modified Proctor hammers following American Society for Testing and Materials (ASTM) D1557 (Standard Test Methods for Laboratory Compaction Characteristics of

Soil Using Modified Effort (56,000 ft-lbf/ft^3 (2,700 kN-m/m^3))), as displayed in Figure 3-9. After compaction, each specimen was extruded from the compaction mold, sealed in a labeled plastic bag, and placed in a large cooler for temperature control and easy transport to the BYU Highway Materials Laboratory for unconfined compressive strength (UCS) testing at specific curing times. A total of 30 to 40 specimens were prepared at each site except for Wyoming, where cement-treated samples were collected from just two stations, neither of which corresponded to the stations tested with the portable instruments during microcracking.

After the cement was mixed into the base material, the CTB was compacted using a vibratory roller. The size of the compactor varied with pulverization depth; the CTB materials at the sites in Utah were mixed to a depth of 8 in. and compacted using an 8-ton vibratory roller, while the CTB material at the Wyoming sites was mixed to a depth of 9 in. and compacted using a 12-ton vibratory roller. As illustrated in Figure 3-10, the roller closely followed the reclaimer at each site to ensure that the freshly mixed CTB would be compacted quickly.

Figure 3-9: Compacting field specimens.

Figure 3-10: Mixing and compacting CTB layer.

3.2.3 Testing Procedures

The CTB was tested for stiffness at each of the 10 stations at each site immediately after final compaction using the CIST, PFWD, and SSG, as shown in Figures 2-6 to 2-8, respectively. Three readings from each instrument were recorded at each station.

In addition, DCP and nuclear density gauge (NDG) tests were performed immediately after final compaction to characterize the CTB material at each station, with the exception of the Wyoming sites where DCP and NDG tests were performed at locations that did not correspond to the other test stations due to constraints caused by limited resources and rapid construction procedures. DCP tests were performed immediately after compaction at each of the sites located in Utah and 3 days after CTB compaction at each of the Wyoming sites. Depicted in Figure 3-11, NDG testing was performed to measure the dry density and moisture content of the CTB layer. The radioactive source was positioned in every case 2 in. above the bottom of the CTB

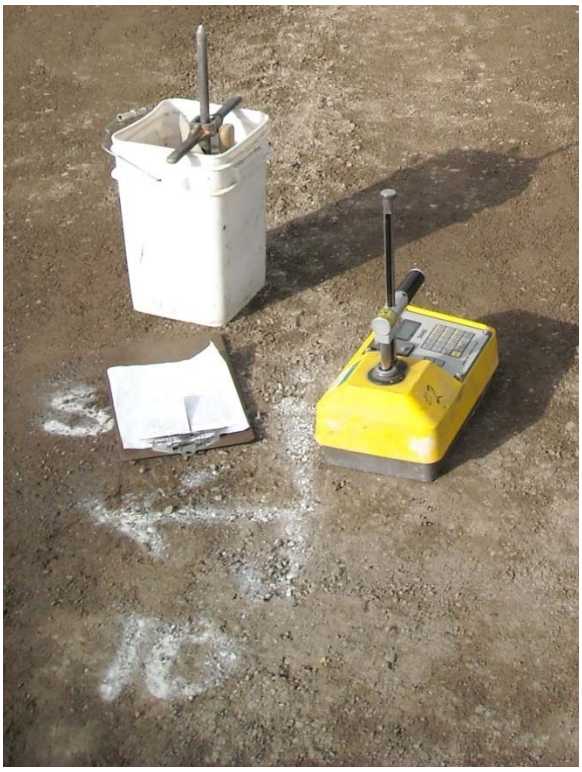

Figure 3-11: NDG testing.

layer. At each of the Utah sites, NDG testing was performed at the same 10 stations tested using the other instruments. At the Wyoming site, 163 NDG tests were performed across the project.

Proper curing of the CTB after final compaction was ensured with the use of water trucks. Frequent watering of the CTB surface maintained relatively moist conditions ideal for cement hydration.

Microcracking of the CTB was performed 2 to 5 days after construction of the CTB, depending on the cement hydration rate and corresponding strength gain of the CTB, using the same vibratory roller employed for compaction. Microcracking was performed after 2 days at Redwood Drive and after 3 days at the Dale Avenue and Wyoming sites. At Spanish Fork, the CTB layer was constructed during a 2-day period but microcracked all on the same day

following 3 days of rain; thus, microcracking at this site was performed after 4 or 5 days following CTB construction, depending on the section of road.

During the microcracking process, the target reduction in stiffness of the composite pavement structure, including the CTB and subgrade, was 40 percent at all the Utah sites and 25 percent at the Wyoming sites using the PFWD; a lower target was applied to the Wyoming sites because that roadway was not scheduled to receive an asphalt surface course for several months, and the researchers were concerned that full microcracking might compromise the performance of the CTB under the heavy truck trafficking typical of that facility. Consistent with the objectives of this research, however, data were also collected using the CIST and SSG. Three measurements were taken with each instrument at each station before microcracking and after each individual vibratory roller pass. Exceptions occurred at the Spanish Fork and Wyoming sites, however, where the necessity of rapidly developing microcracking protocols for the contractor prohibited data collection after each vibratory roller pass at each station. As a minimum effort at the Wyoming project, a new station labeled "Station 11" was created at a convenient location at which measurements after each pass of the vibratory roller were taken for quality control purposes.

An 8-ton vibratory roller was used to microcrack the CTB at all of the Utah sites, while a 12-ton vibratory roller was used at the Wyoming sites. The vibratory rollers were generally operated at a speed of 2 to 3 mph on the sites investigated in this research, which is consistent with current recommendations (Sebesta 2006). During microcracking, the researchers notified the contractor to discontinue vibratory rolling once the target reduction was reached. The resulting CIST, PFWD, and SSG data were statistically analyzed to determine the sensitivity of

each of the portable instruments to microcracking and to determine correlations between each of the three instruments during microcracking.

3.3 Laboratory Testing

The material samples retrieved from the field were returned to the BYU Highway Materials Laboratory for testing. Several material characterization tests were performed on the pre-treatment samples, while UCS testing was performed on the post-treatment samples, as described in the following sections.

3.3.1 Material Characterization

The material characterization tests performed at the BYU Highway Materials Laboratory include determinations of moisture content, asphalt content, and RAP content; sieve analyses; and material classification for each site, with the exception of Wyoming where no material samples were collected for moisture content or sieve analyses due to limited resources and rapid construction procedures at that site. Upon being delivered to the laboratory, each of the 10 pre-treatment RAP-base samples collected from individual stations was divided into three fractions to facilitate these tests. The first fraction was weighed before and after oven-drying at 140°F for a period of 48 hours to determine the moisture content, which was computed as a percentage of the dry aggregate weight of the sample; a temperature of 140°F was used to minimize volatilization of the asphalt present in RAP.

The second fraction of each sample of pre-treatment RAP-base blend was subjected to sieve analysis. The sample was oven-dried at 140°F and separated over 10 different sieve sizes in general accordance with ASTM D422 (Standard Test Method for Particle-Size Analysis of

Soils), with the exception that washing was not performed: 3/4 in., 1/2 in., 3/8 in., No. 4, No. 8, No. 16, No. 30, No. 50, No. 100, and No. 200 sieves, in addition to the pan. To ensure that each sieve analysis was performed with less than a 1 percent sample mass loss, the total weight retained on each of the sieves and pan was compared with the original weight of the sample. The fineness modulus (FM) was calculated from the results of the dry sieve analyses by adding together the cumulative percent retained values for the following sieves and then dividing by 100: 3/4 in., 1/2 in., 3/8 in., No. 4, No. 8, No. 16, No. 30, No. 50, and No. 100.

The same fraction subjected to sieve analysis was subsequently subjected to burn-off testing to measure the asphalt content of the sample. A sample of neat asphalt collected from each site was also tested. In both cases, the samples were first oven-dried at 140°F to eliminate any moisture contained in the samples to avoid mistaking asphalt weight loss with moisture weight loss. The samples were then placed in a burn-off oven at a temperature of 1000°F following ASTM D6307 (Standard Test Method for Asphalt Content of Hot-Mix Asphalt by Ignition Method) until a stable weight was achieved. The asphalt content was subsequently calculated as a percentage of the original weight of the total sample. The RAP content for a given RAP-base blend was determined by dividing the asphalt content in the RAP-base blend by the asphalt content in the neat asphalt sample collected from the corresponding site. Because a neat asphalt sample was not collected from the Spanish Fork site, the RAP content could not be calculated for those stations.

The third fractions of all of the pre-treatment RAP-base samples from a given site were combined together, and a subsample of that mixture was then subjected to washed sieve analyses, hydrometer testing, and Atterberg limits testing. Washed sieve and hydrometer analyses were conducted in general accordance with ASTM D422 to determine the particle-size

distribution of the given samples. Atterberg limits tests were used to assess the plasticity of the samples following ASTM D4318 (Standard Test Methods for Liquid Limit, Plastic Limit, and Plasticity Index of Soils). These results were used to classify the RAP-base blends at each site using both the American Association of State Highway and Transportation Officials (AASHTO) method and the Unified Soil Classification System (USCS) following AASHTO M145 (Classification of Soil and Soil-Aggregate Mixtures for Highway Construction Purposes) and ASTM D2487 (Standard Practice for Classification of Soils for Engineering Purposes (Unified Soil Classification System)), respectively.

3.3.2 Strength Testing

The manually compacted field specimens were cured at room temperature in sealed plastic bags for specific curing times corresponding to the day of microcracking of the CTB layer in the field, which ranged from 3 to 5 days after final compaction of the CTB, and 7 days, 28 days, 6 weeks, or 9 months if a sufficient number of compacted specimens remained for additional testing. Curing in this manner was chosen to simulate an ideal condition of moist-curing in the field. After curing, the height and weight of the specimens were measured, and each sample was then capped using high-strength gypsum to create flat and level specimen ends as pictured in Figure 3-12. After the gypsum caps hardened, UCS tests were performed at a constant strain rate of 0.05 in./minute according to ASTM D1633 (Standard Test Methods for Compressive Strength of Molded Soil-Cement Cylinders). A specimen in the compression machine is shown in Figure 3-13. The strength of the specimen was then computed by dividing the maximum measured load by the cross-sectional area of the specimen. Each specimen was then oven-dried at 140°F to enable calculation of moisture content and dry density. For the Utah

sites, one sample from each station was tested at a given curing time, while three or four samples were tested at each curing time for the Wyoming site.

Figure 3-12: Capping field specimens.

Figure 3-13: UCS testing.

3.4 Statistical Analysis

To meet the objectives of this research, several linear regression analyses were performed on the data collected using the CIST, PFWD, and SSG during the microcracking process. The average of the three readings from each instrument was taken as a single observation at each station and testing time for use in these analyses.

To evaluate the sensitivity of each instrument to microcracking, the average percent change at each station was compared to the number of passes of the vibratory roller using a linear regression analysis. This analysis was performed separately for each site. To compare measurements of CTB stiffness reduction obtained using the three devices, the average percent change in stiffness measured with each instrument at each station was compared to the average percent change in stiffness measured with each of the other instruments, again using a linear regression analysis. In this case, all sites were simultaneously analyzed. For all of the regression analyses performed in this research, various data transformations were considered to improve the interpretation of the statistical results; however, the transformations did not yield improved statistical models and were therefore not applied in the final regression analyses.

The results of the regression analyses included both *p*-values and coefficients of determination, or R^2 values. For this research, the *p*-values generated in the statistical analyses were compared to the standard error rate of 0.05, where *p*-values less than or equal to 0.05 indicated statistical significance. The R^2 value is a measure of how well a given regression equation fits the observed data; an R^2 value of 1.0 represents a perfect model.

3.5 Summary

This research focused on evaluating the sensitivity of the CIST, PFWD, and SSG to microcracking of CTB layers and comparing measurements of CTB stiffness reduction obtained using the three devices. The test locations included in this study were Redwood Drive and Dale Avenue in Salt Lake City, Utah; 300 South in Spanish Fork, Utah; and a private access road in Wyoming.

Properties of the original base and subgrade were obtained by testing those layers using a DCP and by sampling the existing material for laboratory testing. Experimental testing in the field consisted of randomized stationing at each site; sampling the CTB immediately after the cement was mixed into the reclaimed base material; compacting specimens for laboratory testing; and testing the CTB immediately after construction, immediately before microcracking, immediately after each pass of the vibratory roller during the microcracking process, and, in some instances, three days after microcracking. Several laboratory material characterization tests were later performed on the pre-treatment samples, while UCS testing was performed on the post-treatment samples.

Microcracking of the CTB was performed 2 to 5 days after construction of the CTB, depending on the cement hydration rate and corresponding strength gain of the CTB, using the same vibratory roller employed for compaction. During the microcracking process, the target reduction in stiffness of the composite pavement structure, including the CTB and subgrade, was 40 percent at all the Utah sites and 25 percent at the Wyoming sites using the PFWD.

Several linear regression analyses were performed after data were collected using the CIST, PFWD, and CIST during the microcracking process to meet the objectives of this research. The average of the three readings from each instrument was taken as a single

observation at each station and testing time for use in these analyses. The results of the regression analyses included both *p*-values and R^2 values. For this research, the *p*-values generated in the statistical analyses were compared to the standard error rate of 0.05.

4 RESULTS

4.1 Overview

The results of this research include site characterization data, microcracking data, and statistical analyses as described in the following sections. The results from each of the nine sites are presented in the following order in each section: Redwood Drive, Dale Avenue, Spanish Fork, and Wyoming. Depending on the type of data presented, the Wyoming reconstruction project is either referred to as one single project or as six sites labeled Wyoming A through F. In all tables throughout this chapter, the presence of a hyphen indicates that the data were not measured, were not available, or could not be calculated.

4.2 Site Characterization

Site characterization data include in-situ moisture content, cement content, asphalt content, RAP content, bulk sieve analyses, and soil classification. Tables 4-1 to 4-4 specifically present in-situ moisture content, cement content, asphalt content, and RAP content for each of the site locations. The average value, standard deviation, and coefficient of variation are included in each table. The average moisture content of the pre-treatment material ranged from 4.4 to 6.0 percent across the sites. The cement content for the sites where cement slurry was used ranged from 3.8 to 5.0 percent, which is within 1 percent of the target cement content. The

average RAP content, which was obtained from the average asphalt content for each site, ranged from 11 to 38 percent.

Table 4-1: Pre-Treatment Data for Redwood Drive

Station	Moisture content (%)	Cement content (%)	Asphalt content (%)	RAP content (%)
1	4.3	6.0	2.9	46
2	3.8	2.7	2.3	35
3	3.8	2.0	2.3	37
4	3.8	1.5	3.0	47
5	3.6	3.9	0.4	6
6	7.6	3.8	2.3	36
7	4.3	5.6	1.1	18
8	4.2	5.9	2.0	32
9	4.1	5.8	1.8	28
10	4.9	1.2	2.3	36
Average	4.4	3.8	2.0	32
Std. dev.	1.2	1.9	0.8	12
CV (%)	26.4	49.8	38.3	38

Table 4-2: Pre-Treatment Data for Dale Avenue

Station	Moisture content (%)	Cement content (%)	Asphalt content (%)	RAP content (%)
1	5.0	8.5	3.4	64
2	5.2	3.2	3.2	61
3	3.5	7.0	2.9	53
4	5.5	1.3	2.7	50
5	5.7	4.4	2.4	45
6	4.1	6.3	3.3	62
7	3.4	5.0	3.0	55
8	3.6	1.6	3.0	56
9	3.1	5.8	2.7	50
10	6.0	4.3	2.7	51
Average	4.5	4.8	2.9	55
Std. dev.	1.1	2.3	0.3	6
CV (%)	23.7	48.4	11.2	11

Table 4-3: Pre-Treatment Data for Spanish Fork

Station	Moisture content (%)	Cement content (%)	Asphalt content (%)	RAP content (%)
1	6.8	12.3	1.8	-
2	8.0	1.0	1.6	-
3	5.1	10.9	1.9	-
4	6.5	0.4	2.0	-
5	4.3	-	1.6	-
6	6.3	1.8	1.6	-
7	5.0	5.5	2.0	-
8	5.8	-	2.0	-
9	5.7	0.3	1.9	-
10	6.2	8.2	1.9	-
Average	6.0	5.0	1.8	-
Std. dev.	1.1	4.9	0.2	-
CV (%)	17.7	97.2	9.2	-

Table 4-4: Pre-Treatment Data for Wyoming

Station	Moisture content (%)	Cement content (%)	Asphalt content (%)	RAP content (%)
240+00	-	-	5.1	48
206+00	-	-	6.5	62
Average	-	-	5.8	55
Std. dev.	-	-	1.0	9
CV (%)	-	-	17.1	17

Among the properties included in these tables, cement content, in particular, warrants further explanation. The cement content for each station where cement slurry was applied was determined from the weight of cement collected in each sampling pan, the water content of the cement slurry, the depth and width of each mixing path, and the dry density of the base material. Based on the target cement content of 4 percent, Redwood Drive was not sufficiently stabilized. However, researchers found that the catch pans used for capturing the cement slurry from the mixer trucks did not accurately represent the cement application on the base course because of the inconsistent flow rate of slurry exiting the cement chute; the researchers on site observed that the cement slurry would exit the mixing drum in surges. The use of a slurry box created a

smoother rate of cement slurry distribution; however, the pans were again not adequate for collecting a representative sample because of the varying location of the orifice valves passing over the catch pans. As a result, the cement contents are not necessarily considered accurate representations of in-situ conditions.

The results of dry sieve analyses are displayed in Tables 4-5 to 4-7 and Figures 4-1 to 4-3; the legend in each figure designates the test stations. The FM was computed for each gradation as a quantitative measure of particle-size distribution. The FM values for each site where sieve analyses were performed are given in Table 4-8.

The results of the washed sieve analyses are displayed in Table 4-9 and Figure 4-4. All of the tested materials were determined to be non-plastic. Based on these results, the AASHTO classifications of the blended base material for Redwood Drive, Dale Avenue, and Spanish Fork were determined to be A-1-b, A-1-a, and A-1-b, respectively; the corresponding USCS classifications were determined to be silty gravel with sand, well-graded gravel with silt and sand, and silty sand with gravel.

Table 4-5: Dry Sieve Analysis Data for Redwood Drive

Sieve size	Percent passing (%)										Average	Std. dev.	CV (%)
	Station												
	1	2	3	4	5	6	7	8	9	10			
3/4 in.	83.8	84.9	90.6	90.0	91.9	90.7	90.6	88.5	91.0	89.5	89.2	2.7	3.0
1/2 in.	77.6	80.9	83.5	79.7	90.2	82.2	86.6	80.2	83.9	80.7	82.6	3.7	4.5
3/8 in.	72.1	76.8	79.0	74.0	87.3	73.1	80.0	74.2	79.1	74.6	77.0	4.5	5.9
No. 4	58.2	63.1	64.5	60.1	73.6	52.8	64.5	57.1	65.5	59.1	61.8	5.7	9.3
No. 8	44.9	49.5	49.3	46.8	55.3	35.9	48.1	40.4	52.5	44.9	46.8	5.6	12.1
No. 16	32.3	35.0	35.3	32.9	40.1	23.2	34.3	26.5	38.5	32.6	33.1	5.1	15.3
No. 30	23.4	23.8	25.8	22.8	30.9	16.5	25.6	18.1	27.4	24.5	23.9	4.2	17.5
No. 50	15.5	14.5	17.1	14.5	23.1	11.6	18.0	11.7	16.8	17.1	16.0	3.3	20.8
No. 100	9.0	7.8	9.6	8.1	14.8	8.1	11.1	7.1	8.7	10.6	9.5	2.3	23.9
No. 200	3.9	3.3	2.2	1.5	4.1	4.1	3.9	3.5	3.3	4.3	3.4	0.9	26.6
Pan	0.0	0.0	0.0	0.0	0.0	0.0	0.0	0.0	0.0	0.0	-	-	-

Table 4-6: Dry Sieve Analysis Data for Dale Avenue

Sieve size	Percent passing (%)										Average	Std. dev.	CV (%)
	Station												
	1	2	3	4	5	6	7	8	9	10			
3/4 in.	83.9	79.4	80.1	78.1	77.3	77.0	75.9	82.9	86.1	80.4	80.1	3.3	4.1
1/2 in.	74.0	70.8	70.5	69.3	66.9	68.3	67.3	72.9	77.5	70.9	70.9	3.3	4.6
3/8 in.	66.4	64.4	64.1	62.7	59.9	62.9	61.1	66.5	71.4	64.5	64.4	3.2	5.0
No. 4	48.9	47.6	47.6	45.9	42.6	46.3	46.1	48.5	52.9	46.6	47.3	2.6	5.6
No. 8	33.7	33.0	34.4	31.5	28.5	31.8	33.2	33.9	35.8	31.3	32.7	2.0	6.2
No. 16	22.8	21.9	23.5	21.3	17.7	21.8	23.1	23.8	24.1	20.6	22.1	1.9	8.6
No. 30	16.1	14.8	15.4	14.9	10.4	15.6	16.2	17.3	16.5	14.2	15.1	1.9	12.4
No. 50	11.0	9.8	9.5	9.9	6.7	10.7	10.8	12.0	11.0	9.9	10.1	1.4	13.9
No. 100	5.5	3.9	5.1	5.6	3.0	3.3	2.5	2.5	2.5	2.7	3.7	1.3	35.5
No. 200	0.7	0.2	0.2	0.4	0.2	0.1	0.1	0.1	0.0	0.1	0.2	0.2	98.5
Pan	0.0	0.0	0.0	0.0	0.0	0.0	0.0	0.0	0.0	0.0	-	-	-

Table 4-7: Dry Sieve Analysis Data for Spanish Fork

Sieve size	Percent passing (%)										Average	Std. dev.	CV (%)
	Station												
	1	2	3	4	5	6	7	8	9	10			
3/4 in.	90.8	87.5	89.7	95.2	89.4	85.3	89.9	86.8	93.3	92.1	90.0	3.0	3.4
1/2 in.	84.3	78.5	81.9	90.5	80.6	81.8	80.1	77.7	86.9	85.5	82.8	4.0	4.8
3/8 in.	64.4	70.2	73.7	82.8	73.1	76.3	71.2	69.3	76.7	77.6	73.5	5.1	7.0
No. 4	42.0	53.5	56.3	63.3	56.6	65.3	53.9	50.3	58.1	59.4	55.9	6.6	11.8
No. 8	38.4	40.8	44.0	50.2	45.3	56.5	42.9	38.2	43.6	45.8	44.6	5.5	12.3
No. 16	26.9	30.3	34.2	39.1	34.8	46.7	33.7	28.5	30.8	33.4	33.9	5.7	16.8
No. 30	17.1	19.6	23.8	25.4	22.8	32.4	23.7	19.5	19.3	21.8	22.5	4.3	19.1
No. 50	7.5	7.1	12.0	12.5	11.7	14.0	13.2	10.5	10.2	10.2	10.9	2.3	21.0
No. 100	3.7	4.2	4.5	4.8	4.8	4.8	5.6	4.4	4.2	4.2	4.5	0.5	11.4
No. 200	1.6	1.8	1.4	1.6	1.7	1.7	2.0	1.6	1.6	1.8	1.7	0.1	8.9
Pan	0.0	0.0	0.0	0.0	0.0	0.0	0.0	0.0	0.0	0.0	-	-	-

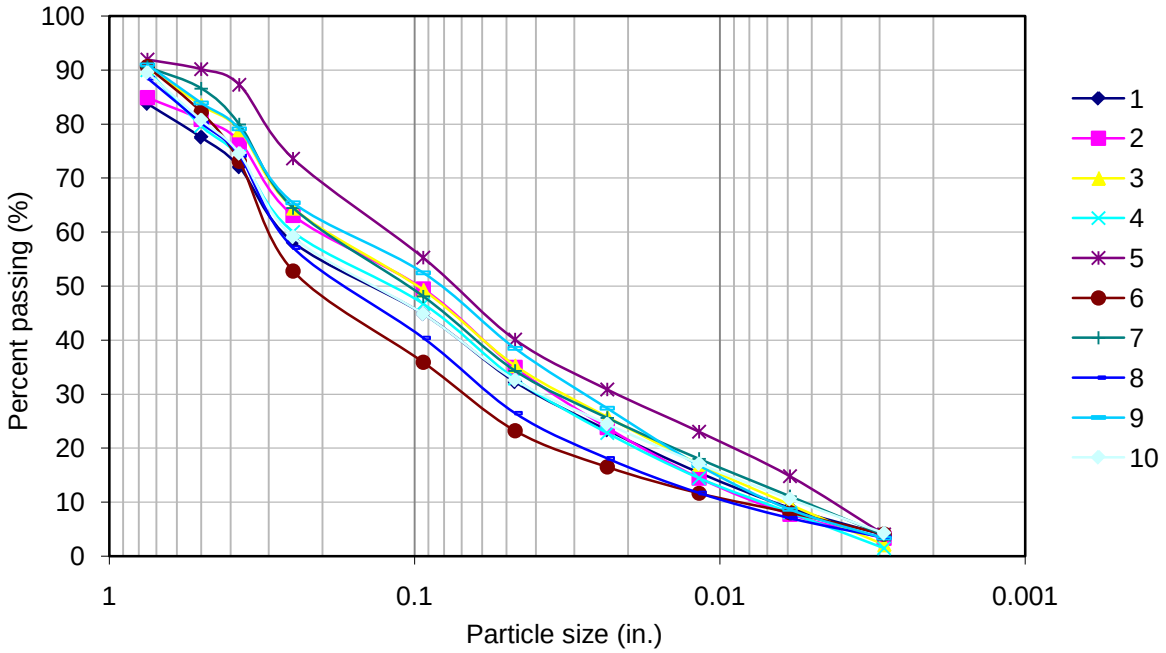

Figure 4-1: Dry sieve analysis data for Redwood Drive.

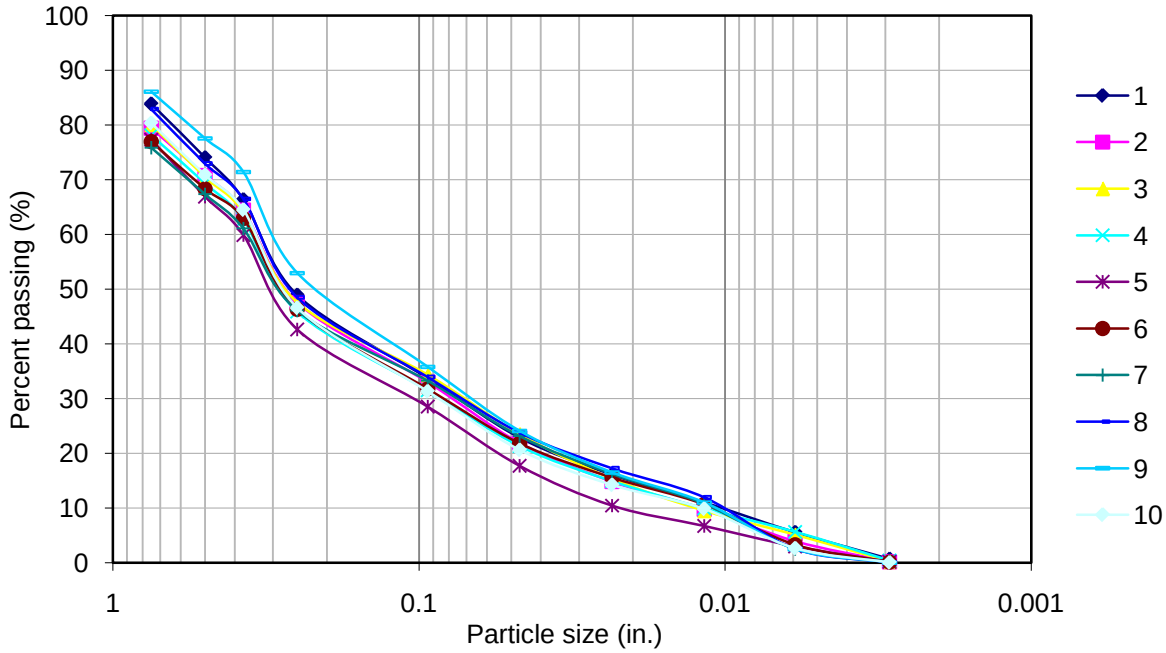

Figure 4-2: Dry sieve analysis data for Dale Avenue.

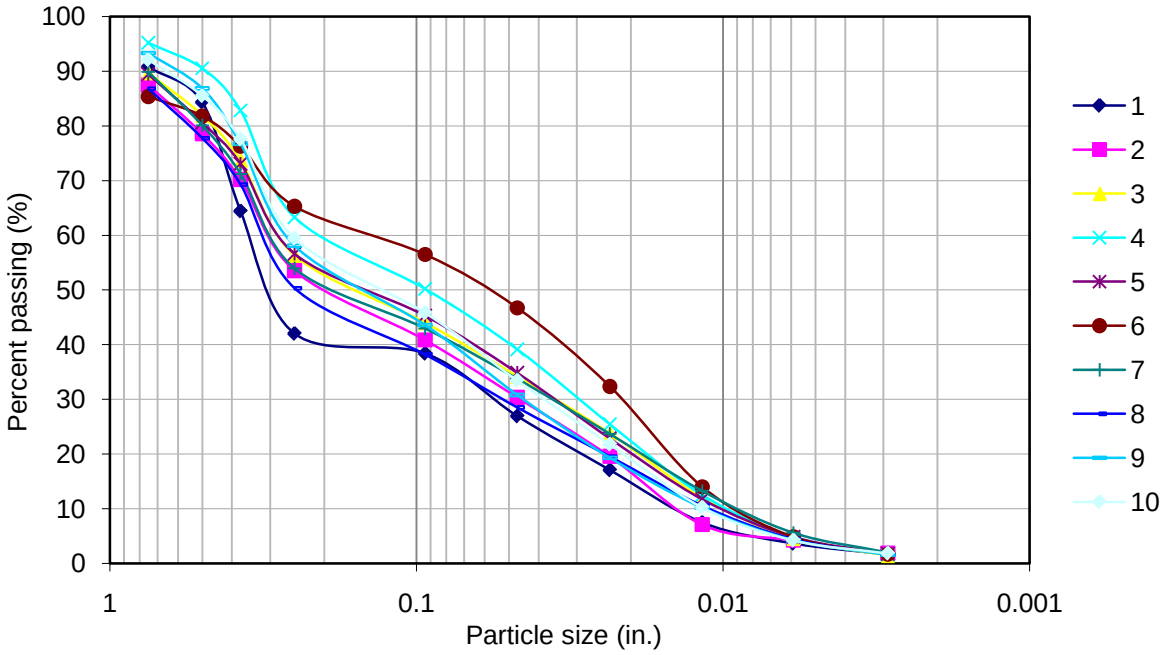

Figure 4-3: Dry sieve analysis data for Spanish Fork.

Table 4-8: FM Values for Redwood Drive, Dale Avenue, and Spanish Fork

Station	Fineness modulus		
	Red.Dr.	Dale Ave.	Sp. Fork
1	4.83	5.38	5.25
2	4.64	5.54	5.08
3	4.45	5.50	4.80
4	4.71	5.61	4.36
5	3.93	5.87	4.81
6	5.06	5.62	4.37
7	4.41	5.64	4.86
8	4.96	5.40	5.15
9	4.37	5.22	4.77
10	4.66	5.59	4.70
Average	4.60	5.54	4.81
Std. dev.	0.33	0.18	0.30
CV (%)	7.15	3.19	6.16

Table 4-9: Washed Sieve Analysis and Hydrometer Data

Sieve size	Red. Dr.		Dale Ave.		Sp. Fork	
	Particle size (in.)	Percent passing (%)	Particle size (in.)	Percent passing (%)	Particle size (in.)	Percent passing (%)
3/4 in.	0.750	89.2	0.750	74.2	0.750	90.2
1/2 in.	0.500	79.6	0.500	68.0	0.500	84.7
3/8 in.	0.375	72.2	0.375	62.8	0.375	77.8
No. 4	0.250	57.1	0.250	51.0	0.250	62.7
No. 8	0.094	42.5	0.094	38.8	0.094	52.8
No. 16	0.047	33.2	0.047	30.2	0.047	46.5
No. 30	0.023	26.7	0.023	23.4	0.023	39.8
No. 50	0.012	23.0	0.012	18.6	0.012	29.2
No. 100	0.006	19.0	0.006	14.6	0.006	20.8
No. 200	0.003	14.1	0.003	10.7	0.003	14.7
	0.00268	13.7	0.00290	10.6	0.00290	14.7
	0.00193	11.9	0.00211	9.9	0.00214	12.8
	0.00143	10.9	0.00153	9.3	0.00159	11.1
	0.00107	9.5	0.00114	8.0	0.00116	9.9
	0.00079	8.6	0.00084	6.7	0.00084	8.9
	0.00057	7.7	0.00062	5.6	0.00061	7.8
Hydrometer	0.00042	7.1	0.00046	4.9	0.00045	7.2
	0.00031	6.2	0.00033	4.3	0.00032	6.7
	0.00022	5.4	0.00024	3.7	0.00023	6.4
	0.00016	4.8	0.00017	3.2	0.00017	5.3
	0.00012	4.1	0.00012	2.6	0.00012	4.8
	0.00008	3.4	0.00009	2.4	0.00008	4.3
	0.00005	2.5	0.00005	2.0	0.00005	3.6

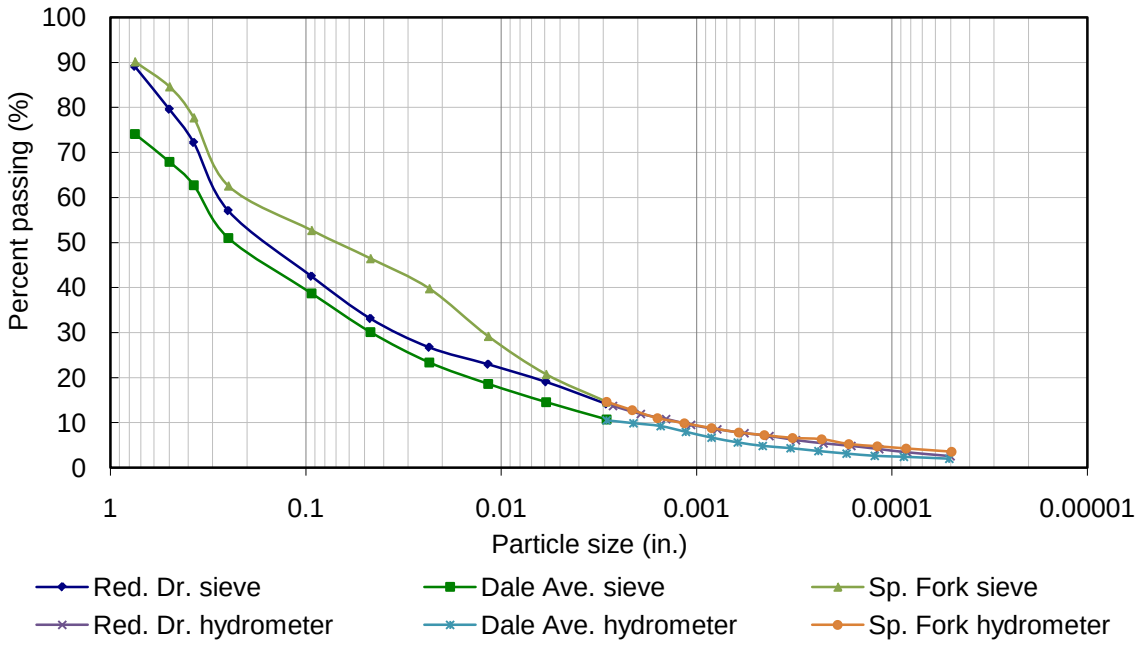

Figure 4-4: Washed sieve analysis and hydrometer data.

4.2.1 Pavement Properties before Reconstruction

CBR values for the base and subgrade prior to reconstruction of Redwood Drive, Spanish Fork, and Wyoming are displayed in Table 4-10 to 4-12, respectively; BYU researchers were unable to perform DCP tests on the original pavement structure at Dale Avenue. The depth of DCP penetration into the subgrade is also given in the tables. Because the locations tested before and after reconstruction were not the same at the Spanish Fork and Wyoming sites, the station numbering used for pre-construction testing does not correspond to the station numbering used during post-construction CIST, PFWD, and SSG testing at those sites.

Table 4-10: DCP Data for Redwood Drive before Reconstruction

Station	Base CBR (%)	Subgrade CBR (%)	Penetration into subgrade (in.)
1	41.1	21.2	20.0
2	61.6	9.5	20.2
3	74.9	8.2	19.2
4	70.4	12.0	19.4
5	70.9	11.2	18.8
6	59.8	12.4	20.9
7	68.3	10.5	19.4
8	133.0	9.9	18.6
9	98.7	8.9	19.8
10	57.2	10.1	18.7
Average	73.6	11.4	19.5
Std. dev.	25.5	3.7	0.7
CV (%)	34.7	32.4	3.8

Table 4-11: DCP Data for Spanish Fork before Reconstruction

Station	Base CBR (%)	Subgrade CBR (%)	Penetration into subgrade (in.)
1	78.3	10.2	18.4
2	65.7	30.3	16.6
3	57.7	27.6	15.8
4	64.0	56.7	17.7
5	72.5	43.1	17.2
6	33.1	17.4	17.3
Average	61.8	30.9	17.2
Std. dev.	15.8	17.0	0.9
CV (%)	25.5	54.9	5.0

Table 4-12: DCP Data for Wyoming before Reconstruction

Station	Base CBR (%)	Subgrade CBR (%)	Penetration into subgrade (in.)
1	8.4	15.2	10.0
2	32.5	5.3	9.8
3	41.1	14.2	7.3
4	31.5	5.8	15.7
5	23.2	5.5	15.1
6	28.7	7.4	9.4
7	22.1	7.5	17.8
8	46.9	12.2	14.2
9	34.7	8.0	13.9
10	45.9	4.6	12.9
11	22.4	2.4	14.5
12	46.2	5.7	16.0
13	32.0	3.5	12.3
14	25.1	6.3	17.0
15	71.2	19.5	7.2
Average	31.5	8.6	12.6
Std. dev.	11.8	3.9	3.3
CV (%)	37.4	45.0	26.4

4.2.2 Pavement Properties after Reconstruction

CBR values for the base and subgrade layers after reconstruction are displayed in Tables 4-13 to 4-16. DCP tests were performed at each site immediately after final compaction of the CTB, except for the DCP test at the Wyoming site that was performed after 3 days of curing as mentioned previously. Several DCP tests were actually attempted at the Wyoming sites; however, the pavement structure was relatively stiff, and only one DCP test was successfully completed. The station reported in Table 4-16 does not correspond with any other station at the Wyoming sites.

At the Redwood Drive and Spanish Fork sites, the average base CBR values of the original pavements were higher than those of the new pavements immediately after construction, as cement hydration in the new pavement structures had not yielded measurable strength

improvements at the time of testing. However, because the CTB layer at the Wyoming site had more time to cure prior to DCP testing, the average base CBR value of the new pavement was substantially higher than that of the original pavement at that location.

Table 4-13: DCP Data for Redwood Drive after Reconstruction

Station	Base CBR (%)	Subgrade CBR (%)	Penetration into subgrade (in.)
1	42.5	6.7	20.9
2	37.5	11.5	19.3
3	29.3	16.0	20.1
4	93.6	30.7	21.2
5	49.2	57.2	19.3
6	36.9	14.2	19.8
7	30.6	21.9	19.8
8	93.5	44.2	20.4
9	24.4	11.4	19.8
10	24.1	12.7	20.7
Average	46.2	22.7	20.1
Std. dev.	26.2	16.5	0.7
CV (%)	56.7	72.7	3.2

Table 4-14: DCP Data for Dale Avenue after Reconstruction

Station	Base CBR (%)	Subgrade CBR (%)	Penetration into subgrade (in.)
1	21.2	7.9	19.7
2	30.9	23.4	21.1
3	36.5	9.2	20.9
4	29.9	8.1	19.4
5	35.8	10.6	18.5
6	78.5	24.7	21.2
7	34.2	10.1	18.3
8	21.4	7.3	20.4
9	47.5	19.8	20.4
10	25.1	7.5	19.8
Average	36.1	12.9	20.0
Std. dev.	16.9	6.9	1.0
CV (%)	46.7	53.9	5.1

Table 4-15: DCP Data for Spanish Fork after Reconstruction

Station	Base CBR (%)	Subgrade CBR (%)	Penetration into subgrade (in.)
1	24.3	21.7	11.3
2	27.4	41.8	10.5
3	78.3	38.6	14.9
4	41.2	17.4	13.9
5	34.6	29.5	10.7
6	31.9	28.9	12.5
7	61.1	37.3	13.1
8	26.9	29.4	11.4
9	69.0	22.8	12.4
10	28.9	26.4	11.8
Average	42.4	29.4	12.2
Std. dev.	19.7	7.9	1.4
CV (%)	46.5	26.7	11.4

Table 4-16: DCP Data for Wyoming after Reconstruction

Station	Base CBR (%)	Subgrade CBR (%)	Penetration into subgrade (in.)
-	142.6	16.4	21.3

The values of in-situ dry density and moisture content measured using the NDG at each station are displayed in Tables 4-17 to 4-20. As mentioned previously, the Wyoming test stations at which NDG testing was performed do not correspond to those at which CIST, PFWD, and SSG testing was performed. On average, the values of dry density and moisture content for the Redwood Drive, Dale Avenue, and Spanish Fork sites are relatively close, while the average dry density for the Wyoming site is at least 10 pcf less than the values for the other sites. In addition, the moisture content measured for the Wyoming project is 4 percent greater than the moisture contents of the other sites.

Table 4-17: NDG Data for Redwood Drive after Reconstruction

Station	Dry density (pcf)	Moisture content (%)
1	128.7	6.6
2	128.2	9.8
3	125.7	7.9
4	129.0	6.9
5	127.1	7.5
6	127.4	8.3
7	123.8	9.2
8	125.3	8.3
9	126.1	6.2
10	127.3	7.2
Average	126.9	7.8
Std. dev.	1.6	1.1
CV (%)	1.3	14.7

Table 4-18: NDG Data for Dale Avenue after Reconstruction

Station	Dry density (pcf)	Moisture content (%)
1	123.8	9.3
2	129.5	8.5
3	117.0	8.4
4	124.1	7.5
5	125.8	6.2
6	130.3	6.5
7	124.9	6.5
8	119.4	8.8
9	120.0	8.1
10	125.5	7.5
Average	124.0	7.7
Std. dev.	4.2	1.1
CV (%)	3.4	13.8

Table 4-19: NDG Data for Spanish Fork after Reconstruction

Station	Dry density (pcf)	Moisture content (%)
1	118.8	6.2
2	122.2	7.1
3	129.0	7.2
4	126.4	6.6
5	129.4	6.5
6	121.1	7.6
7	122.8	6.9
8	129.8	6.8
9	129.5	7.5
10	123.7	7.1
Average	125.3	7.0
Std. dev.	4.1	0.4
CV (%)	3.2	6.3

Table 4-20: NDG Data for Wyoming after Reconstruction

163 test stations	Dry density (pcf)	Moisture content (%)
Average	113.8	11.8
Std. dev.	2.1	1.4
CV (%)	1.8	11.5

4.3 Microcracking

The results of field and laboratory testing performed in connection with microcracking at the research sites are described in the following sections.

4.3.1 Field Testing

The CIST, PFWD, and SSG data collected in this research are presented in tabular format in Appendix A and in graphical format in Figures 4-5 to 4-13. Relative to “0 passes,” percentage change in CIST, PFWD, and SSG measurements after each pass of the vibratory roller during microcracking are presented in tabular format in Appendix B and in graphical format in Figures

4-14 to 4-22. In the tables and figures, negative values indicate a decrease in stiffness, while positive values indicate an increase in stiffness.

Concerning the Wyoming data, the type of bedding sand used for SSG testing at Wyoming A and B immediately prior to microcracking, or at "0 passes," was different than the type of bedding sand used for SSG testing after each vibratory roller pass. The later readings were determined to be inconsistent with the previous readings, and data for these two sites were therefore excluded from the analyses performed in this research. The researchers were not previously aware that SSG measurements are sensitive to different types of bedding sand.

Three to four passes of the vibratory roller were required at Redwood Drive to reach a minimum of 40 percent reduction in base modulus using the PFWD, while only one to two passes were required at Dale Avenue. Four passes of the vibratory roller were applied at the Spanish Fork and Wyoming projects, resulting in average reductions in base stiffness of 40.8 percent at the former and between 13.7 and 26.3 percent at the latter, depending on the specific site. In this research, the percent reduction achieved by a given number of roller passes varied from site to site, demonstrating the difficulty of establishing a fixed number of passes in a microcracking specification intended for general use.

In Figures 4-5 to 4-22, readings taken on the day of CTB construction and 3 days after microcracking are shown where applicable. In each of these cases, the data show that the CTB increased in stiffness during the 3 days following microcracking, indicative of autogenous healing.

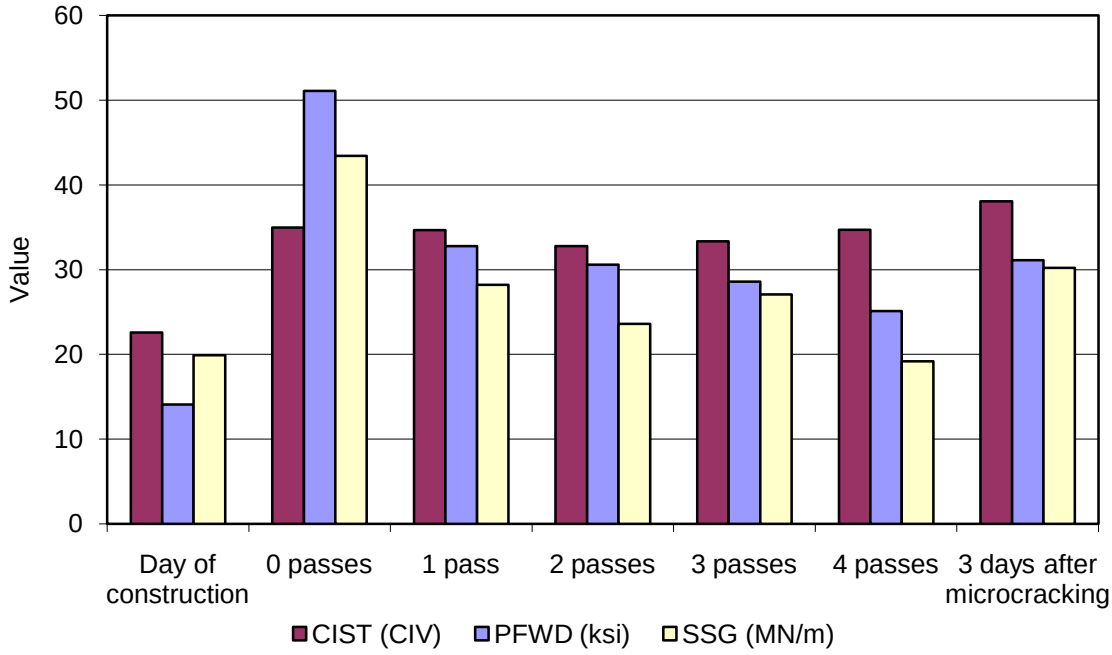

Figure 4-5: Average stiffness measurements at Redwood Drive.

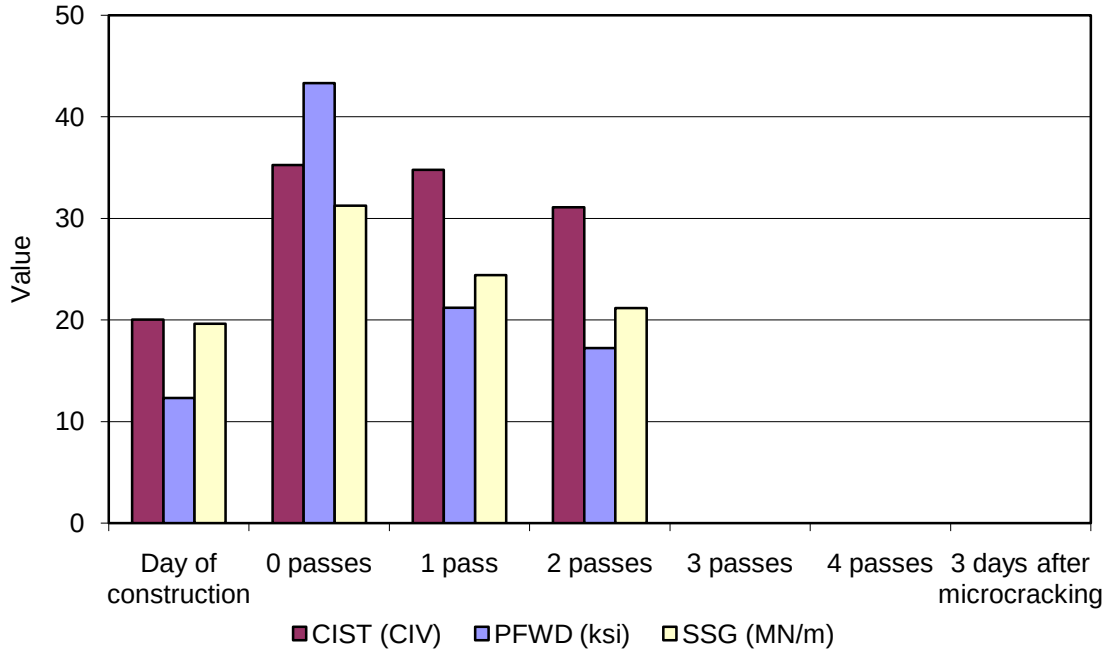

Figure 4-6: Average stiffness measurements at Dale Avenue.

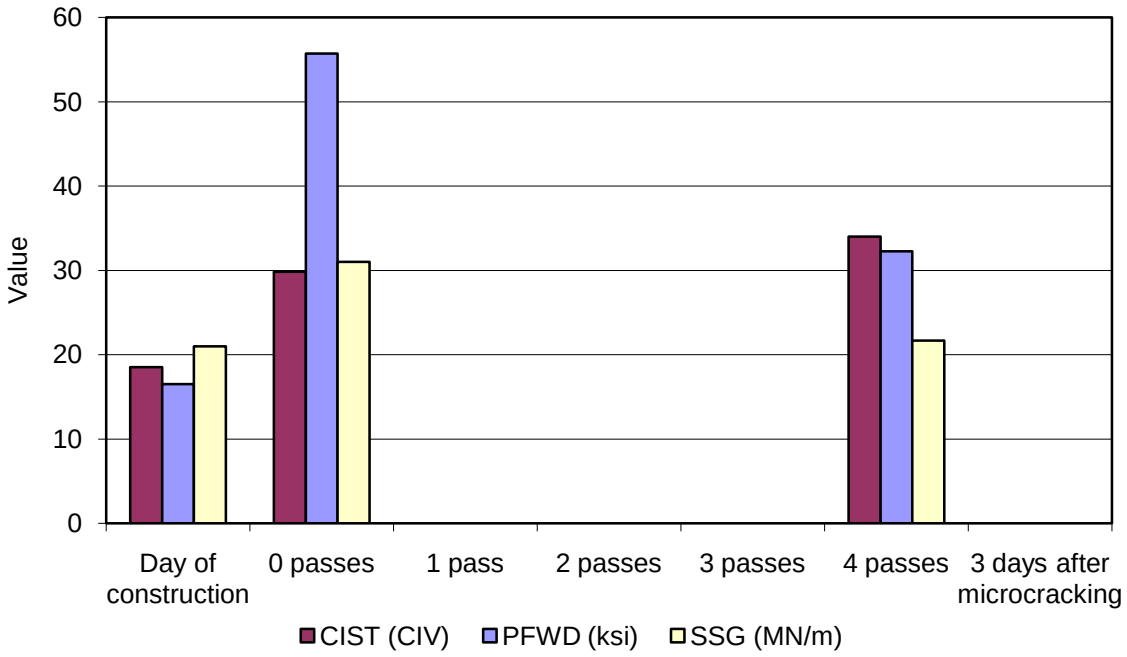

Figure 4-7: Average stiffness measurements at Spanish Fork.

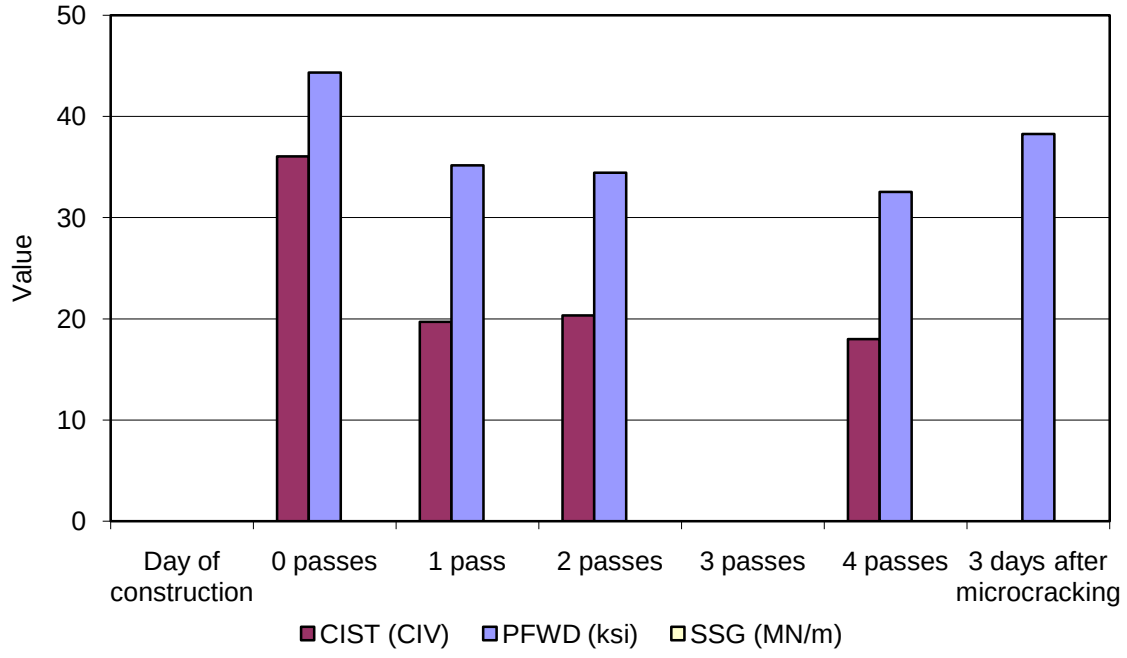

Figure 4-8: Average stiffness measurements at Wyoming A.

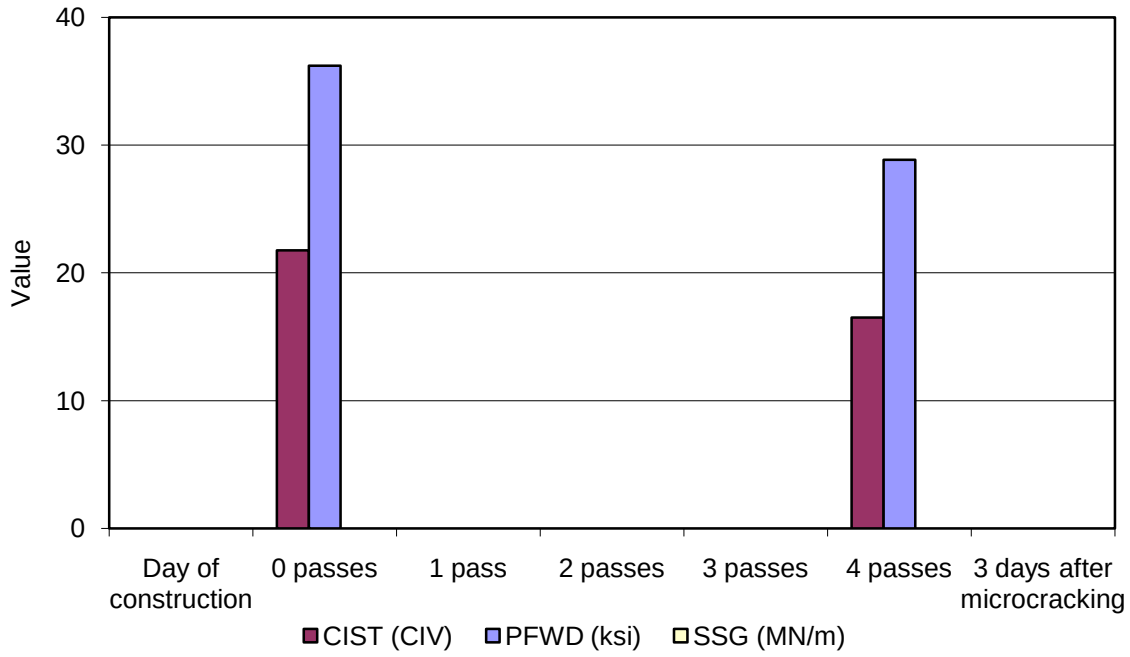

Figure 4-9: Average stiffness measurements at Wyoming B.

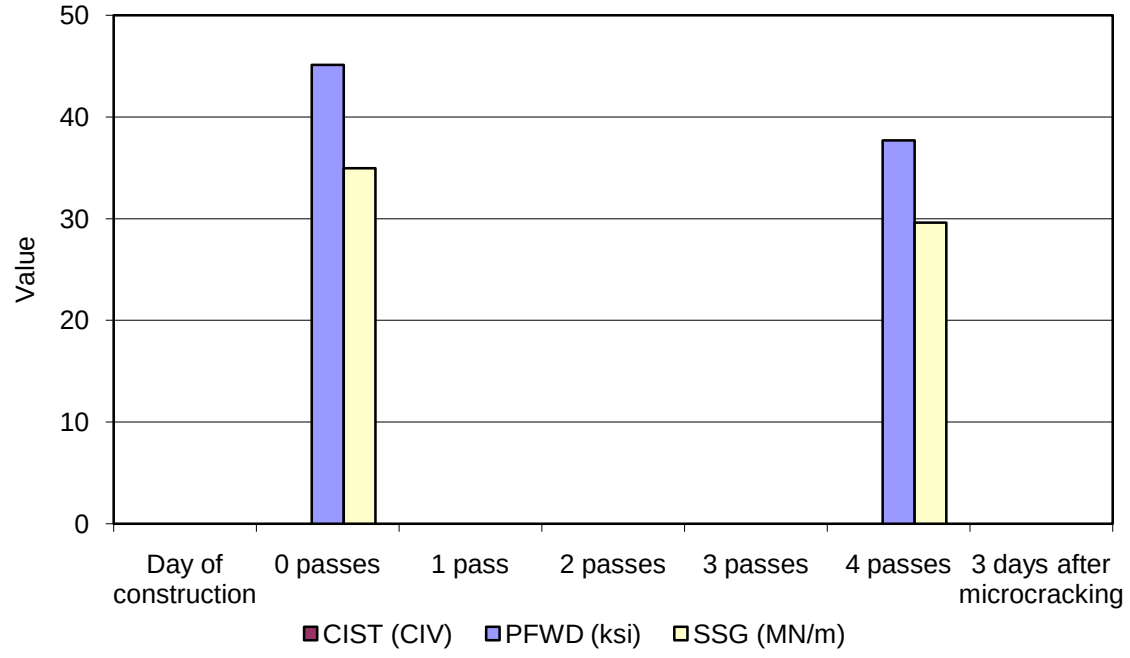

Figure 4-10: Average stiffness measurements at Wyoming C.

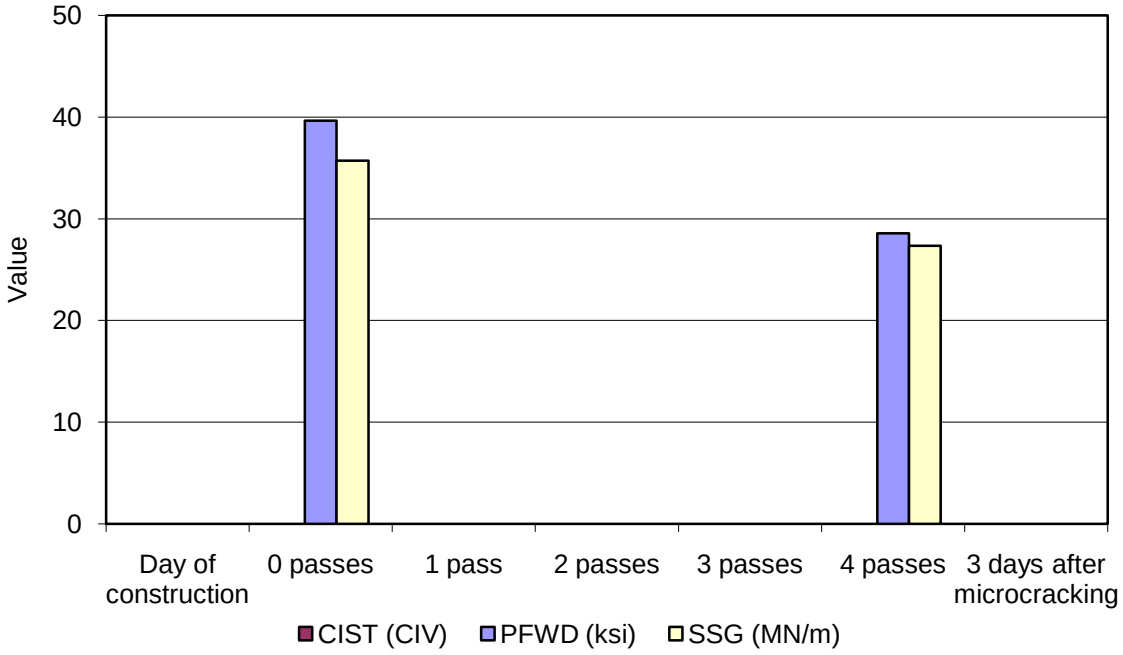

Figure 4-11: Average stiffness measurements at Wyoming D.

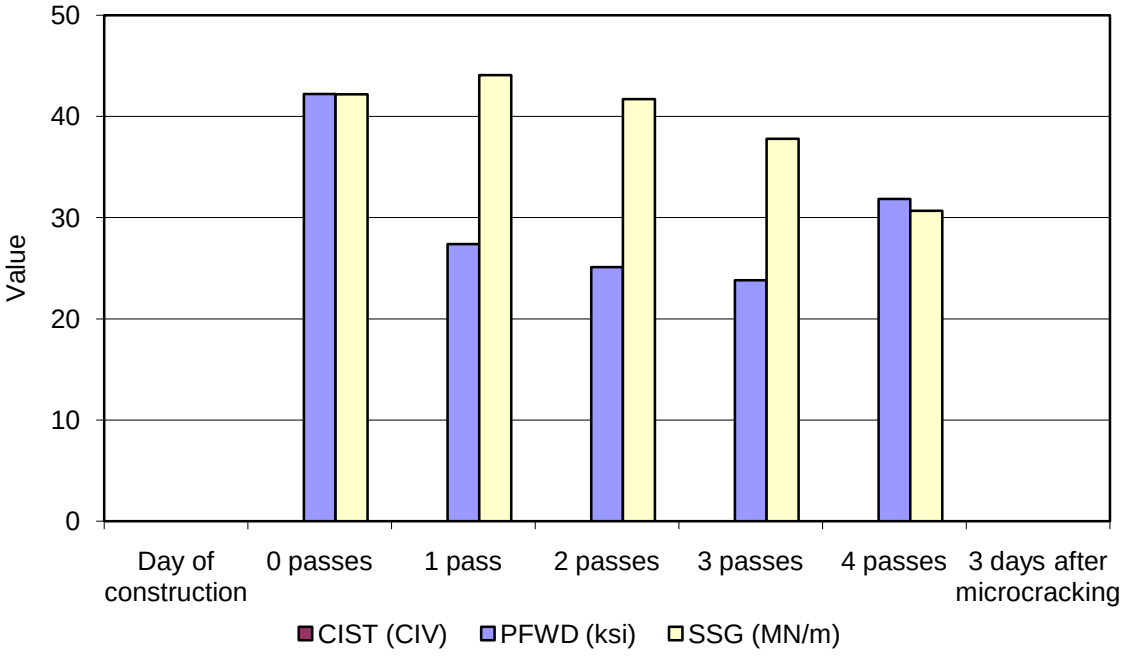

Figure 4-12: Average stiffness measurements at Wyoming E.

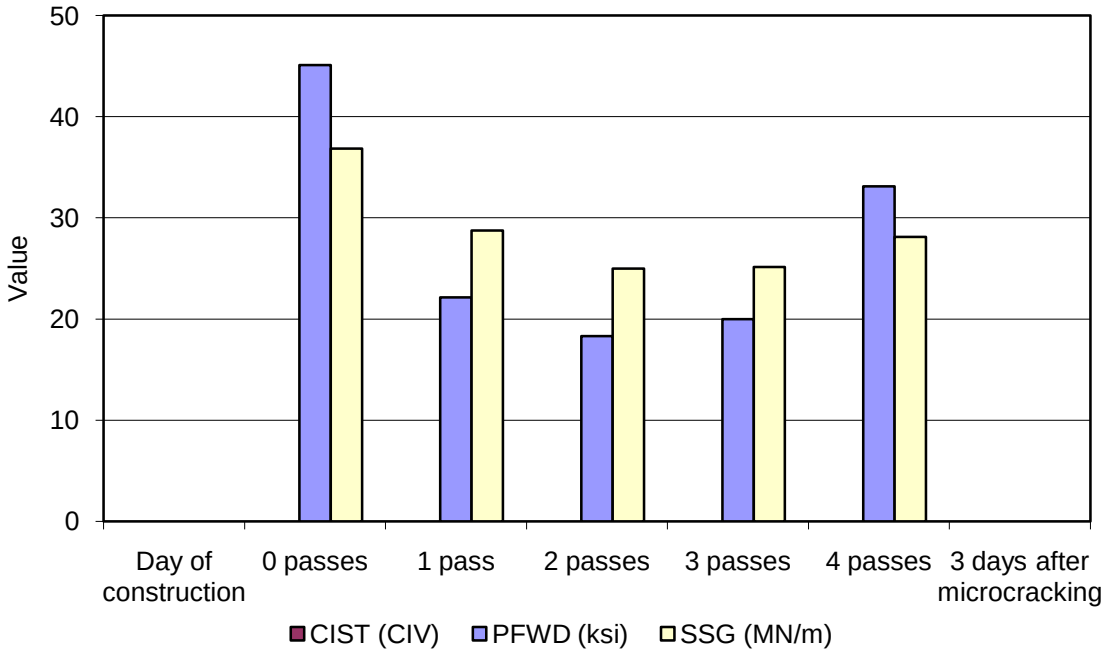

Figure 4-13: Average stiffness measurements at Wyoming F.

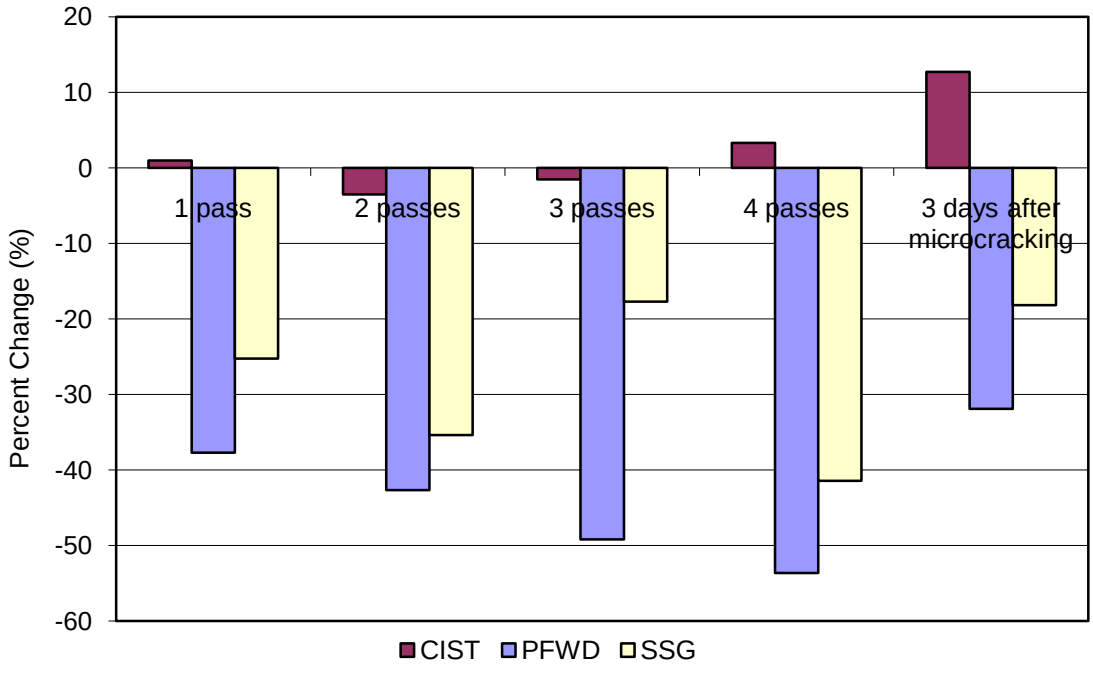

Figure 4-14: Average percent change in stiffness measurements at Redwood Drive.

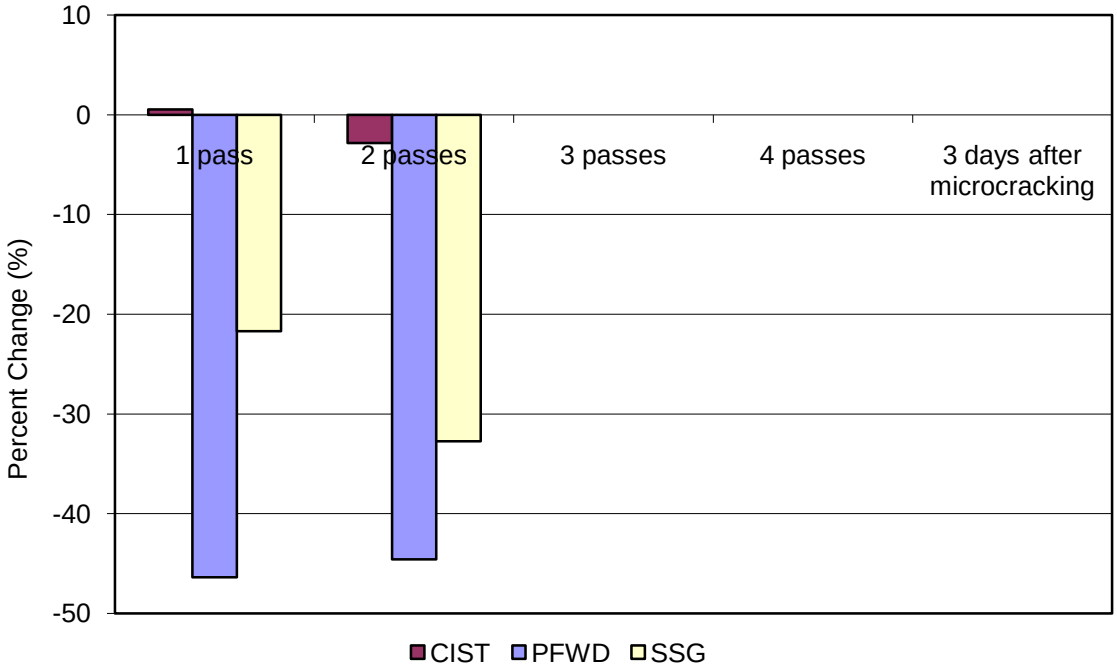

Figure 4-15: Average percent change in stiffness measurements at Dale Avenue.

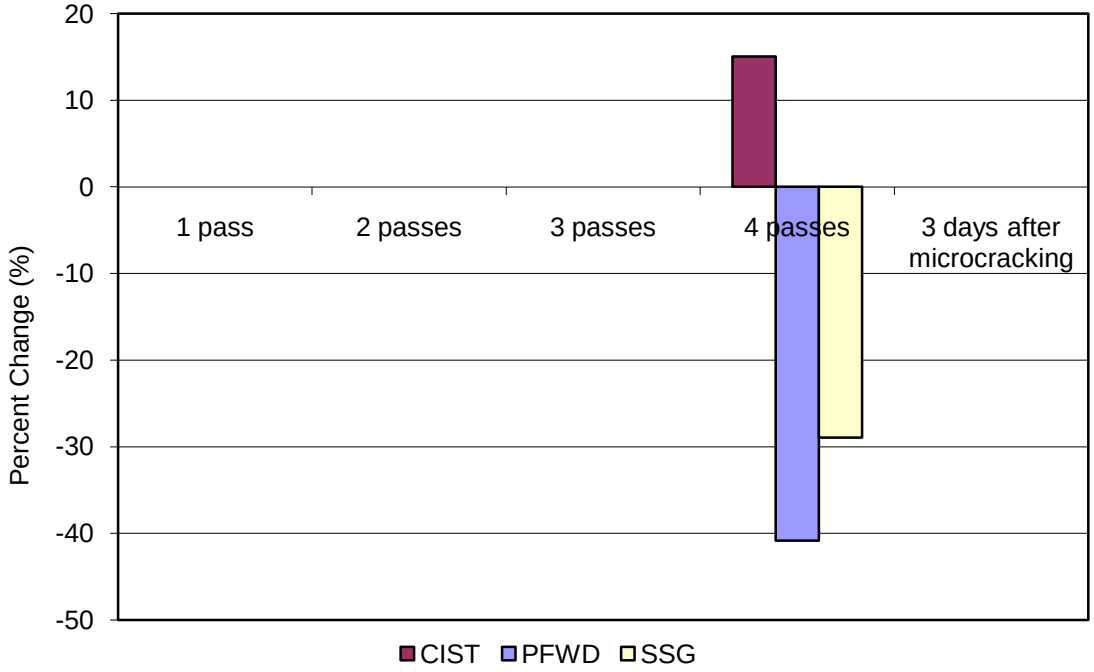

Figure 4-16: Average percent change in stiffness measurements at Spanish Fork.

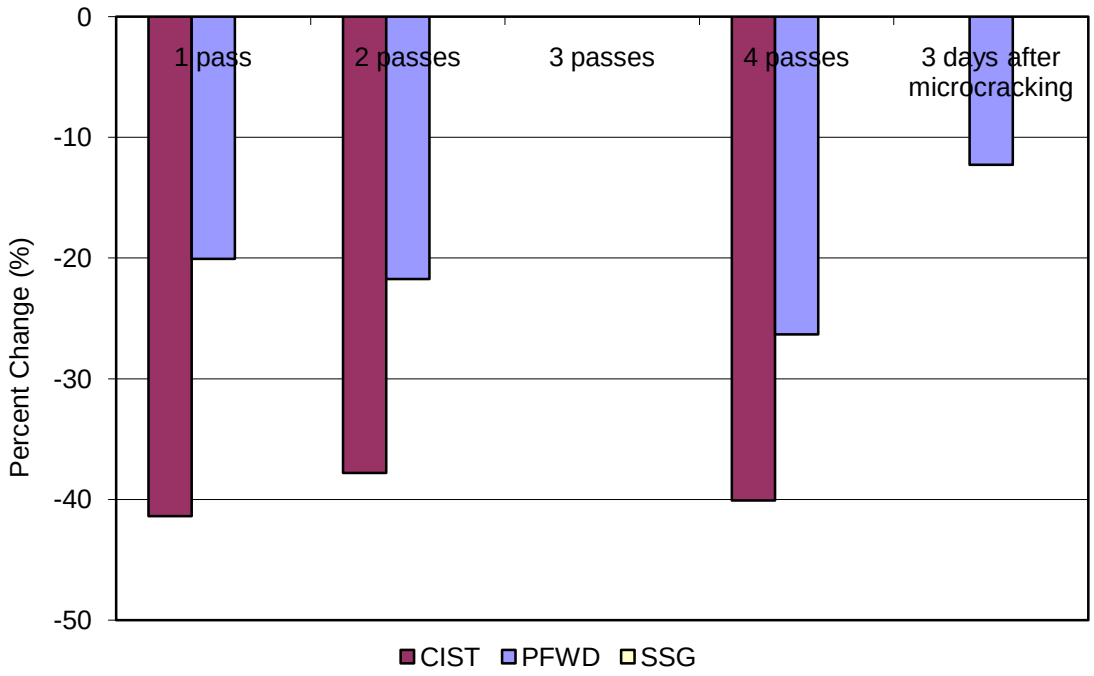

Figure 4-17: Average percent change in stiffness measurements at Wyoming A.

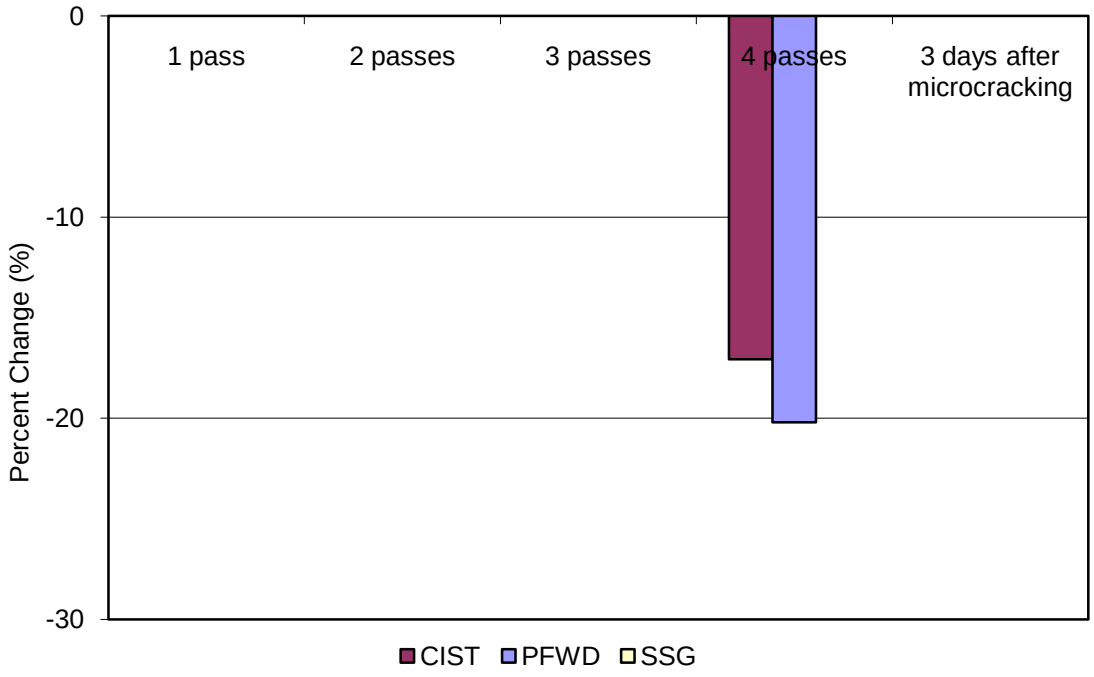

Figure 4-18: Average percent change in stiffness measurements at Wyoming B.

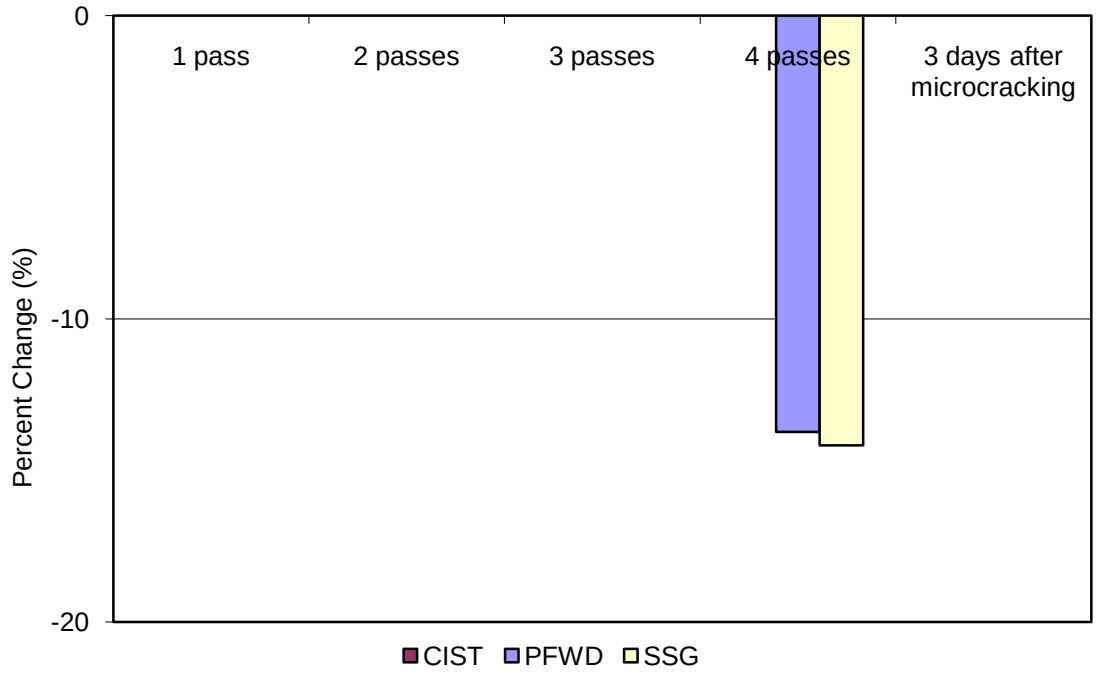

Figure 4-19: Average percent change in stiffness measurements at Wyoming C.

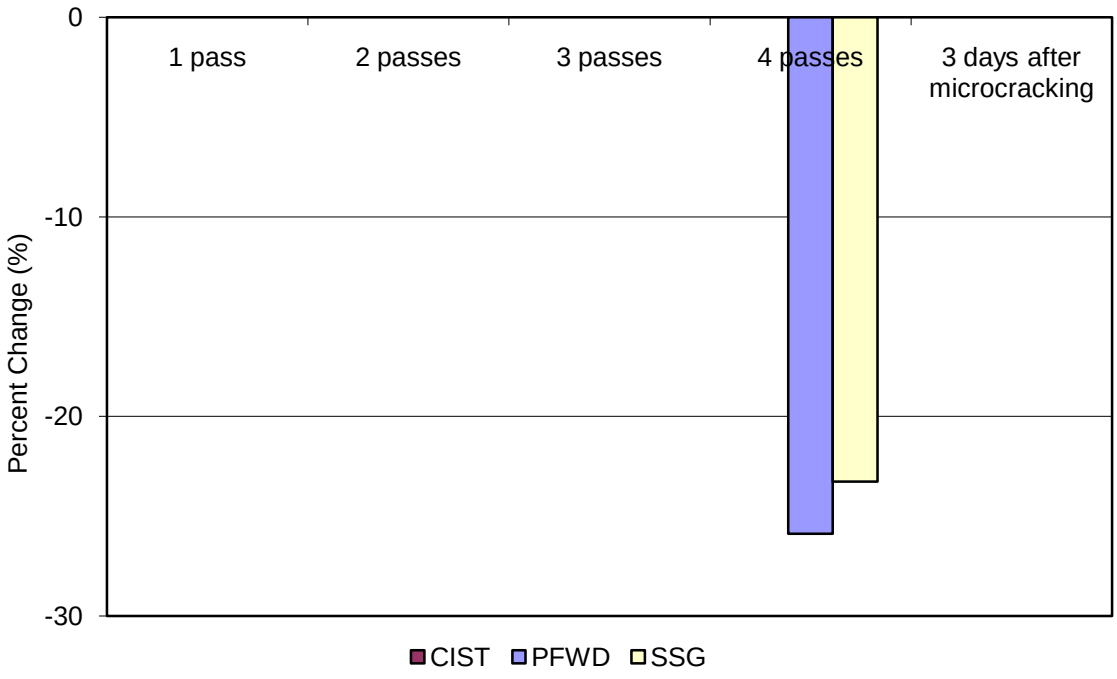

Figure 4-20: Average percent change in stiffness measurements at Wyoming D.

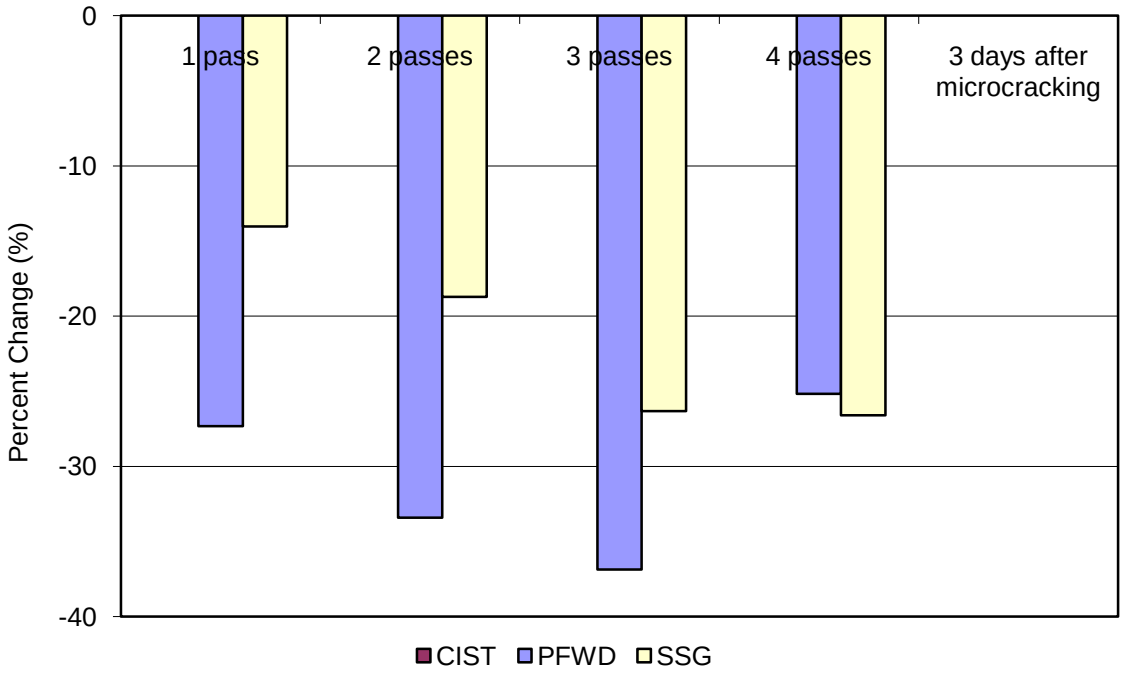

Figure 4-21: Average percent change in stiffness measurements at Wyoming E.

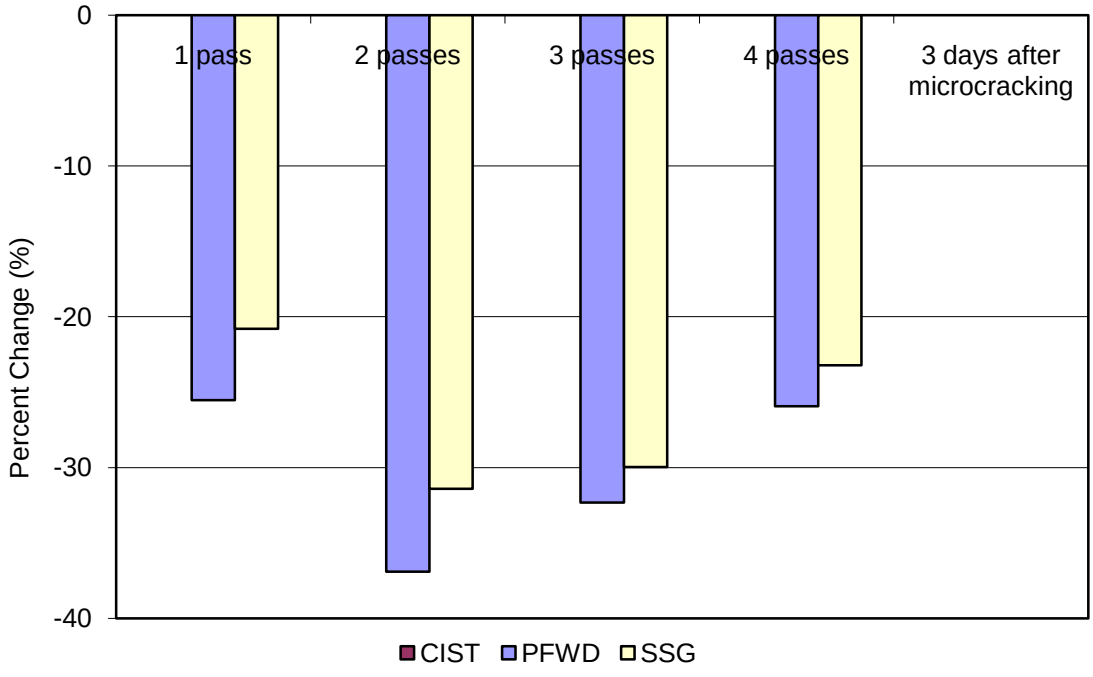

Figure 4-22: Average percent change in stiffness measurements at Wyoming F.

During the process of microcracking, the researchers looked for signs of excessive damage to the CTB. On a few occasions, visible damage to the CTB surface was observed, as shown in Figure 4-23, which indicated that the speed of the roller was too slow or the amplitude of vibration was too high. In these instances, the equipment operator was instructed to increase the roller speed, decrease the amplitude, or discontinue microcracking. On most occasions, however, only fine cracks were noticeable, as shown in Figure 4-24.

4.3.2 Laboratory Testing

Results of the UCS tests performed on the manually compacted field specimens are presented in Tables 4-21 to 4-24. The 2-, 3-, 4-, or 5-day UCS tests were performed in each case at the same time that microcracking was performed at the given site. At the Spanish Fork site,

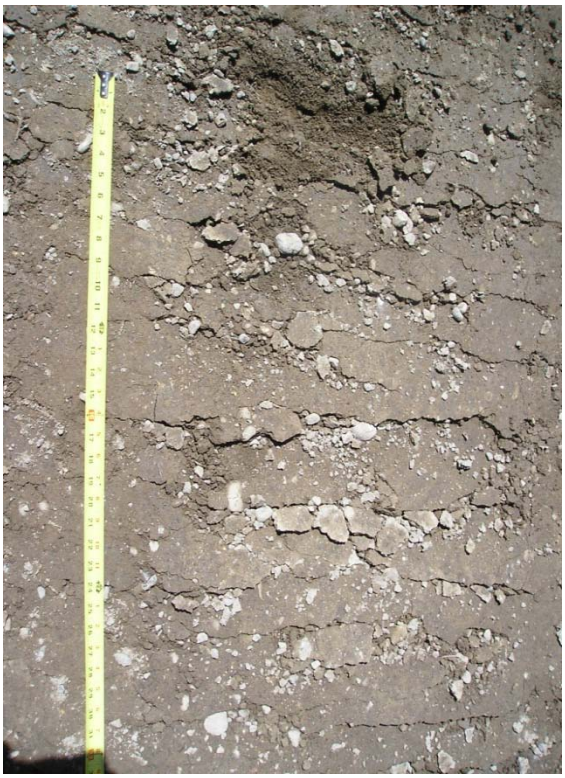

Figure 4-23: CTB surface damage due to slow vibratory roller speed during microcracking.

Figure 4-24: Fine cracks in CTB surface after microcracking.

the CTB construction was performed over a 2-day period, but microcracking of the entire project was performed on a single day. Therefore, because stations 2, 6, and 10 were constructed on the second day, 4-day UCS tests were performed for those stations while 5-day UCS tests were performed for all the other stations. No UCS testing was performed in conjunction with microcracking of the Wyoming sites. According to the results of the UCS tests, the average 7-day CTB strength for each site was consistent with current design recommendations (Luhr et al. 2005). However, because the densities of these manually compacted specimens generally exceeded the in-situ densities measured with the NDG, the actual CTB layers may not have developed the same 7-day strength. The NDG measurements may also have been affected by the presence of RAP in the CTB layer, as the hydrocarbons may have caused artificially high moisture content readings and, in turn, artificially low dry density readings.

Table 4-21: UCS Data for Redwood Drive

Station	UCS (psi)				Dry density (pcf)				Moisture content (%)			
	2-day	7-day	28-day	9-mo.	3-day	7-day	28-day	9-mo.	3-day	7-day	28-day	9-mo.
1	333	429	633	1407	133.7	-	133.2	132.3	7.0	7.5	6.3	2.7
2	364	312	538	1458	131.7	-	133.9	130.5	7.1	7.4	5.8	4.7
3	315	299	477	1266	136.9	-	134.6	137.7	5.6	6.1	5.3	2.9
4	362	364	628	1374	129.4	-	128.5	130.1	7.7	7.4	7.2	5.2
5	1025	963	1978	2483	136.6	-	137.4	138.0	6.3	7.1	5.4	3.7
6	163	95	224	522	132.0	-	133.5	133.9	7.0	7.3	6.8	4.8
7	651	551	1633	1864	130.2	-	135.9	133.2	7.5	7.4	6.1	4.2
8	477	485	778	1465	131.7	-	134.6	135.5	6.9	6.1	6.0	3.2
9	396	407	528	1399	135.9	-	135.5	136.3	5.6	5.0	5.4	3.5
10	395	262	536	1475	133.6	-	132.8	135.6	5.9	6.5	5.2	3.7
Average	448	417	795	1471	133.2	-	134.0	134.3	6.7	6.8	6.0	3.9
Std. dev.	237	230	556	488	2.6	-	2.4	2.8	0.8	0.8	0.7	0.9
CV (%)	53	55	70	33	2.0	-	1.8	2.1	11.3	12.4	11.2	22.2

Table 4-22: UCS Data for Dale Avenue

Station	UCS (psi)			Dry density (pcf)			Moisture content (%)		
	3-day	7-day	28-day	3-day	7-day	28-day	3-day	7-day	28-day
1	-	-	-	-	-	-	-	-	-
2	398	316	593	136.6	134.7	134.6	4.7	5.9	4.8
3	508	451	357	137.4	135.6	135.5	4.4	4.7	4.4
4	361	405	454	135.4	134.8	134.7	4.9	4.9	5.0
5	604	304	907	134.7	137.0	136.9	4.5	4.8	4.4
6	327	556	469	135.0	134.4	134.6	6.0	4.2	5.8
7	436	476	517	132.8	135.6	135.1	4.5	4.7	4.3
8	117	131	181	126.3	128.5	135.4	8.1	8.2	8.4
9	435	402	623	134.5	133.1	133.8	4.8	5.2	4.8
10	259	251	431	133.3	127.6	129.1	6.6	7.7	6.6
Average	383	366	504	134.0	133.5	134.4	5.4	5.6	5.4
Std. dev.	141	129	200	3.2	3.3	2.2	1.3	1.4	1.4
CV (%)	37	35	40	2.4	2.4	1.6	23.5	25.2	25.2

Table 4-23: UCS Data for Spanish Fork

Station	UCS (psi)			Dry density (pcf)			Moisture content (%)		
	4&5-day	7-day	28-day	4&5-day	7-day	28-day	4&5-day	7-day	28-day
1	658	327	890	132.1	130.8	132.0	6.1	6.7	6.3
2	283	341	363	128.9	130.1	128.1	8.1	8.3	8.3
3	783	482	1033	131.9	133.4	133.9	6.6	6.4	6.3
4	390	260	568	130.9	130.6	130.2	6.7	7.2	6.6
5	916	812	969	133.5	129.1	133.2	6.3	6.7	6.2
6	514	450	515	131.0	127.9	128.1	7.8	7.9	7.8
7	669	389	824	133.5	131.5	132.8	6.3	6.3	6.1
8	210	168	237	135.4	131.9	135.1	5.5	5.7	5.6
9	537	399	859	131.1	130.9	129.6	7.1	6.7	6.7
10	376	421	412	130.0	129.3	130.4	8.1	8.0	7.9
Average	534	405	667	131.8	130.5	131.3	6.8	7.0	6.8
Std. dev.	225	171	281	1.9	1.6	2.4	0.9	0.8	0.9
CV (%)	42	42	42	1.5	1.2	1.9	13.1	12.1	13.2

Table 4-24: UCS Data for Wyoming

Station	UCS (psi)		Dry density (pcf)		Moisture content (%)	
	7-day	6-week	7-day	6-week	7-day	6-week
240+00	466	831	116.5	119.6	8.8	7.0
	537	890	118.9	119.3	7.6	6.6
	365	-	117.2	-	8.6	-
	456	-	118.2	-	8.3	-
206+00	325	454	120.5	120.1	7.6	6.6
	355	392	118.2	118.4	7.6	7.2
	349	435	120.1	119.8	7.4	7.0
	316	-	119.0	-	7.9	-
Average	396	600	118.6	119.4	8.0	6.9
Std. dev.	80	239	1.4	0.7	0.5	0.3
CV (%)	20	40	1.1	0.5	6.5	3.7

4.4 Statistical Analysis

The results of sensitivity and correlation analyses are given in the following sections. Only the CIST, PFWD, and SSG readings taken immediately before microcracking and immediately after each vibratory roller pass were evaluated in the statistical analyses performed in this research.

4.4.1 Sensitivity Analysis

Results from the statistical analyses designed to evaluate the sensitivity of each of the three portable instruments to microcracking are presented in Tables 4-25 to 4-27. *P*-values greater than 0.05 indicate that insufficient evidence exists to identify a statistically significant difference in the given base stiffness measurement after each pass of the vibratory roller during the microcracking process. *P*-values less than or equal to 0.05 indicate that the given instrument was sensitive to the microcracking process, or that differences in readings taken between successive passes of the vibratory roller were statistically significant.

Table 4-25: Sensitivity Analysis for the CIST

Station	Sample size	Slope	Intercept	*P*-value	R^2 (%)
Red. Dr.	40	-0.14	0.65	0.925	0.0
Dale Ave.	26	1.22	-0.58	0.693	0.7
Sp. Fork	20	-3.76	0.00	0.017	27.7
WY A	40	7.84	16.10	0.019	13.7
WY B	20	4.27	0.00	0.070	17.1
WY C	-	-	-	-	-
WY D	-	-	-	-	-
WY E	-	-	-	-	-
WY F	-	-	-	-	-

Table 4-26: Sensitivity Analysis for the PFWD

Station	Sample size	Slope	Intercept	*P*-value	R^2 (%)
Red. Dr.	38	12.90	11.70	< 0.001	57.0
Dale Ave.	26	24.70	7.23	< 0.001	66.2
Sp. Fork	20	10.20	0.00	< 0.001	89.3
WY A	40	5.68	7.11	< 0.001	51.4
WY B	20	4.11	0.00	0.008	33.2
WY C	20	3.44	0.00	< 0.001	49.9
WY D	20	6.47	0.00	< 0.001	84.8
WY E	25	6.26	2.46	< 0.001	50.6
WY F	28	6.35	4.26	< 0.001	51.0

Table 4-27: Sensitivity Analysis for the SSG

Station	Sample size	Slope	Intercept	*P*-value	R^2 (%)
Red. Dr.	40	8.49	8.76	< 0.001	32.1
Dale Ave.	26	16.90	1.60	< 0.001	78.9
Sp. Fork	20	7.24	0.00	< 0.001	66.8
WY A	-	-	-	-	-
WY B	-	-	-	-	-
WY C	20	3.55	0.00	< 0.001	50.4
WY D	20	5.81	0.00	< 0.001	93.6
WY E	25	6.64	0.79	< 0.001	80.9
WY F	28	5.75	3.49	< 0.001	59.0

As shown in Table 4-25 for the CIST, three of the five sites have *p*-values greater than 0.05, and all of the R^2 values indicate that variation in the response variable is poorly explained by variation in the predictor variables included in the regression model. The CIST is therefore considered to be insensitive to microcracking. However, as shown in Tables 4-26 and 4-27 for the PFWD and SSG, respectively, all of the *p*-values are less than or equal to 0.05, and several of the R^2 values indicate that variation in the response variable is well explained by variation in the predictor variables included in the regression model. The PFWD and SSG are therefore considered to be sensitive to microcracking.

The difference in sensitivity to microcracking between the three portable instruments may be attributable to the method and zone of interrogation of each instrument. However, studying such differences is beyond the scope of the present research.

4.4.2 Correlation Analysis

Figures 4-25 to 4-27 show plots of the individual data points used in statistical analyses of the CIST-PFWD, CIST-SSG, and PFWD-SSG correlations, and results from these analyses are presented in Table 4-28. *P*-values greater than 0.05 indicate that insufficient evidence exists to identify a statistically significant correlation between the given instruments, while *p*-values less than or equal to 0.05 indicate that a statistically significant correlation exists between the instruments.

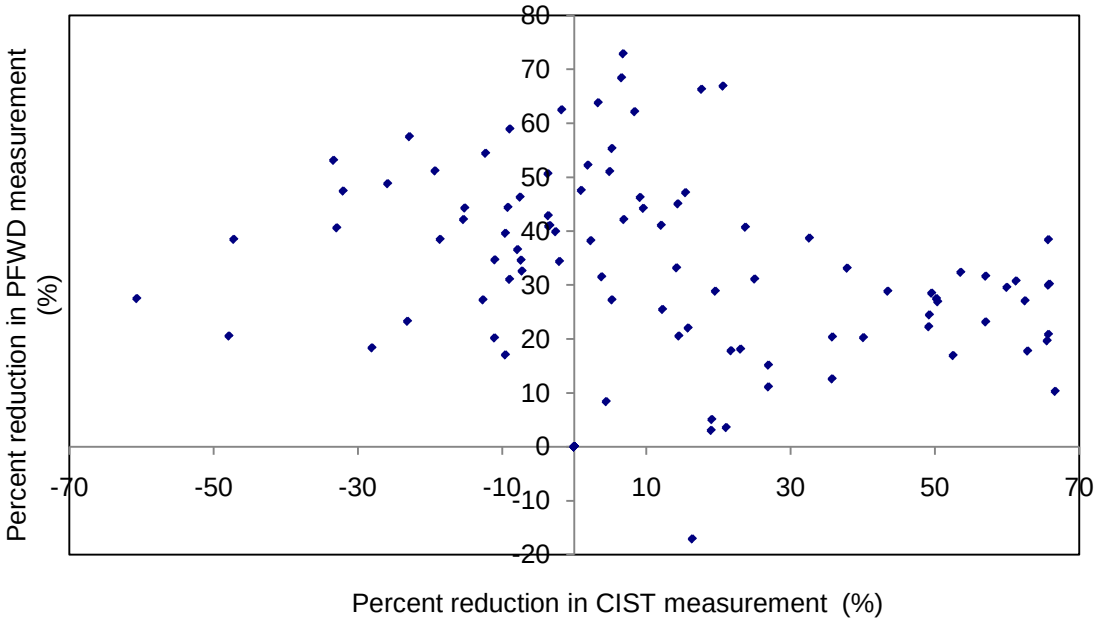

Figure 4-25: Correlation analysis for the CIST and PFWD.

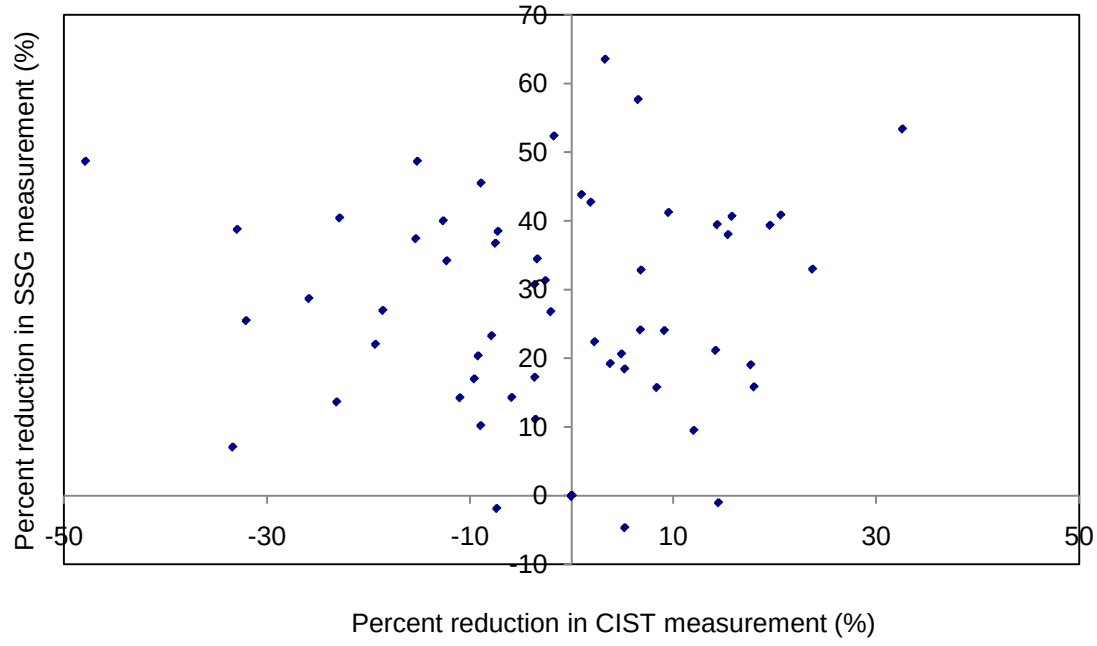

Figure 4-26: Correlation analysis for the CIST and SSG.

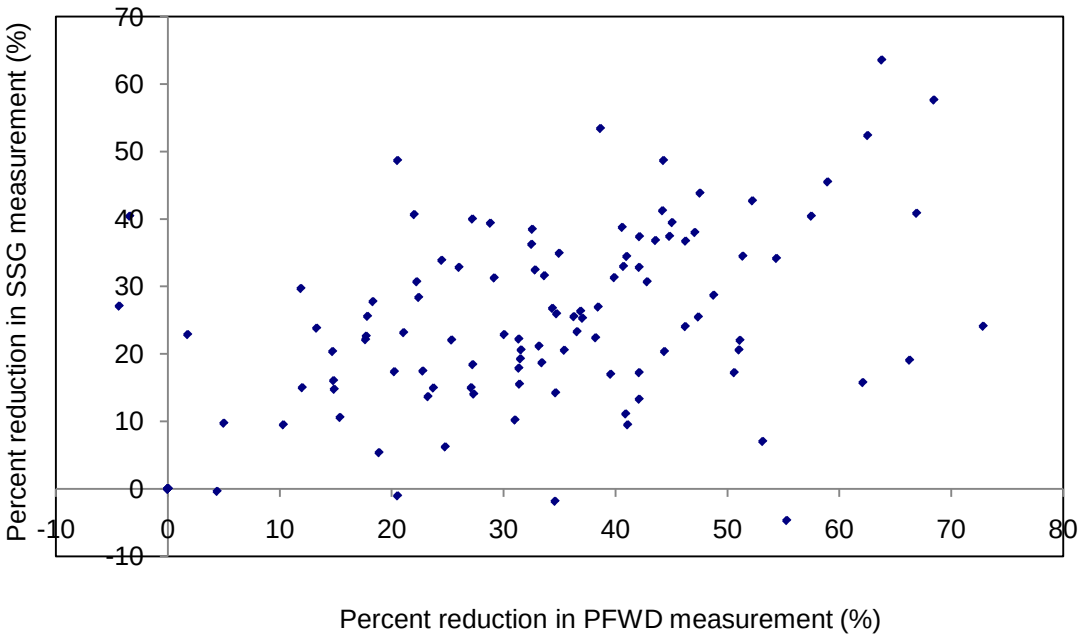

Figure 4-27: Correlation analysis for the PFWD and SSG.

Table 4-28: Correlation Analysis for the CIST, PFWD, and SSG

Instrument	Sample size	Slope	Intercept	*P*-value	R^2 (%)
CIST-PFWD	154	0.01	20.82	0.887	< 0.1
CIST-SSG	86	-0.06	18.58	0.718	< 0.1
PFWD-SSG	167	0.58	3.65	< 0.001	56.4

As shown in Table 4-28, neither of the instrument correlations involving the CIST have *p*-values less than or equal to 0.05; therefore, neither of those correlations are statistically significant. Only the PFWD-SSG correlation has a *p*-value less than or equal to 0.05. Figure 4-28 provides a graphical representation of this correlation in the form of a chart that can be used by engineers and contractors needing to derive target CTB stiffness reductions for one instrument from specified CTB stiffness reductions measured using the other. For example, a target reduction in CTB stiffness of 40 percent using the PFWD equates to a reduction of 27

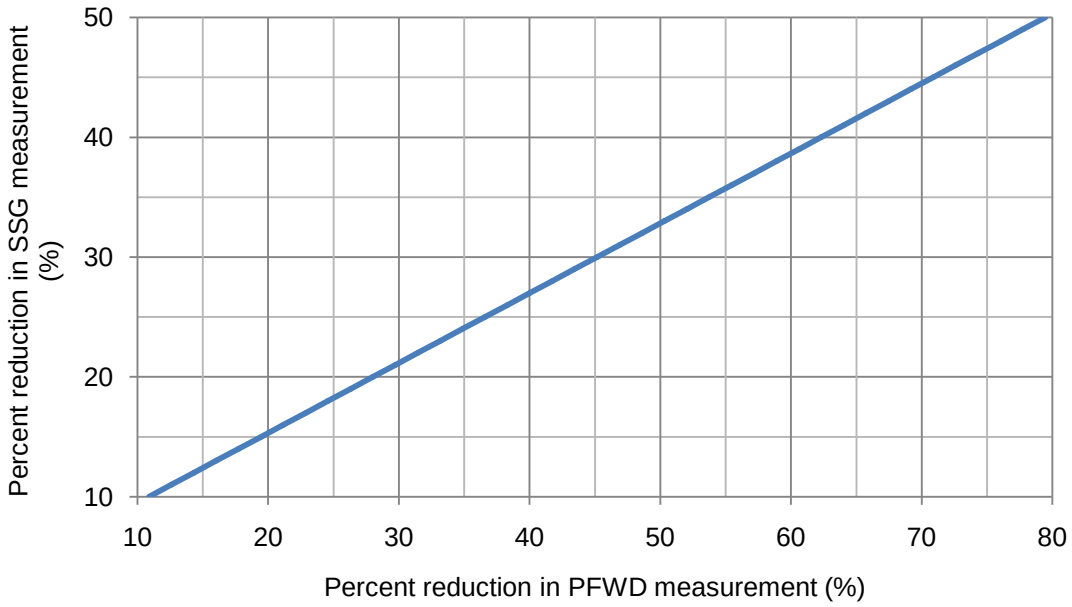

Figure 4-28: Correlation chart for the PFWD and SSG.

percent using the SSG. Use of this chart should enable those with access to only an SSG, which is significantly less expensive than a PFWD, to establish appropriate thresholds for monitoring microcracking with the SSG. The data collected in this research suggest that the heavy CIST should not be used for monitoring microcracking.

4.5 Summary

The results of this research include site characterization data, microcracking data, and statistical analyses. The AASHTO classifications of the blended base material for Redwood Drive, Dale Avenue, and Spanish Fork were determined to be A-1-b, A-1-a, and A-1-b, respectively; the corresponding USCS classifications were determined to be silty gravel with sand, well-graded gravel with silt and sand, and silty sand with gravel.

DCP tests were performed on the original pavement at each site except for Dale Avenue. DCP tests were performed at each site immediately after final compaction of the CTB, except for the DCP test at the Wyoming site that was performed after 3 days of curing as mentioned previously. On average, the values of dry density and moisture content for the Redwood Drive, Dale Avenue, and Spanish Fork sites were relatively close, while the average dry density for the Wyoming site was at least 10 pcf less than the values for the other sites. In addition, the moisture content measured for the Wyoming project was 4 percent greater than the moisture contents of the other sites.

The 2-, 3-, 4-, or 5-day UCS tests were performed in each case at the same time that microcracking was performed at the given site, with the exception of the Wyoming sites. According to the results of the UCS tests, the average 7-day CTB strength for each site was consistent with current design recommendations. However, because the densities of these manually compacted specimens generally exceeded the in-situ densities measured with the NDG, the actual CTB layers may not have developed the same 7-day strength. The NDG measurements may also have been affected by the presence of RAP in the CTB layer, as the hydrocarbons may have caused artificially high moisture content readings and, in turn, artificially low dry density readings.

Two to four passes of the vibratory roller were applied during the microcracking process depending on the site. In this research, the percent reduction achieved by a given number of roller passes varied from site to site, demonstrating the difficulty of establishing a fixed number of passes in a microcracking specification intended for general use.

Results from the statistical analyses designed to evaluate the sensitivity of each of the three portable instruments to microcracking indicate that two of the three portable instruments

studied in this research are sensitive to microcracking. The CIST is considered to be insensitive to microcracking, while both the PFWD and SSG are considered to be sensitive to microcracking. The difference in sensitivity to microcracking between the three portable instruments may be attributable to the method and zone of interrogation of each instrument. However, studying such differences is beyond the scope of the present research.

Neither of the instrument correlations involving the CIST have *p*-values less than or equal to 0.05; therefore, neither of those correlations are statistically significant. Only the PFWD-SSG correlation analysis indicates that a statistically significant correlation exists between the PFWD and SSG. The data collected in this research suggest that the heavy CIST should not be used for monitoring microcracking.

5 CONCLUSION

5.1 Summary

This research focused on evaluating the sensitivity of the CIST, PFWD, and SSG to microcracking of CTB layers and comparing measurements of CTB stiffness reduction obtained using the three devices. The study included four different pavement reconstruction projects in Utah and Wyoming, all of which utilized FDR with cement stabilization. Cement was distributed in slurry form at the Utah projects and in powder form at the Wyoming project. Specified cement contents were all 4 percent by dry weight of aggregate, and the CTB layers ranged in thickness from 6 to 9 in. Field testing was supplemented by laboratory material characterizations on each project.

Microcracking of the CTB was performed 2 to 5 days after construction of the CTB. Two to four passes of the vibratory roller were applied during the microcracking process depending on the site. During the microcracking process, the target reduction in stiffness of the composite pavement structure, including the CTB and subgrade, was 40 percent at all the Utah sites and 25 percent at the Wyoming sites using the PFWD. Three measurements with each instrument were taken at each station before microcracking, between each individual vibratory roller pass, and after microcracking.

Several linear regression analyses were performed after data were collected using the CIST, PFWD, and SSG during the microcracking process to meet the objectives of this research.

The results of the regression analyses included both *p*-values and R^2 values. For this research, the *p*-values generated in the statistical analyses were compared to the standard error rate of 0.05.

5.2 Findings

Results from the statistical analyses designed to evaluate the sensitivity of each of the three portable instruments to microcracking indicate that the PFWD and SSG are sensitive to microcracking, while the CIST is insensitive to microcracking. Results from the statistical analyses designed to compare measurements of CTB stiffness reduction demonstrate that neither of the instrument correlations involving the CIST are statistically significant. Only the correlation between the PFWD and SSG was shown to be statistically significant.

5.3 Recommendations

In this research, the percent reduction achieved by a given number of roller passes varied from site to site, demonstrating the difficulty of establishing a fixed number of passes in a microcracking specification intended for general use. Given the results of this research, engineers and contractors should utilize the PFWD or SSG for monitoring microcracking of CTB layers. Regarding the SSG, a consistent source of bedding sand should be used throughout the microcracking process to obtain reliable results. The heavy CIST is unsuitable for monitoring microcracking and should not be used.

For deriving target CTB stiffness reductions measured using either the PFWD or SSG from specified targets measured using the other, engineers and contractors should utilize the correlation chart developed in this research. The chart shows, for example, that a target reduction in CTB stiffness of 40 percent using the PFWD equates to a reduction of 27 percent

using the SSG. Use of this chart should enable those with access to only an SSG, which is significantly less expensive than a PFWD, to establish appropriate thresholds for monitoring microcracking with the SSG.

REFERENCES

Adaska, W. and Luhr, D., "Control of Reflective Cracking in Cement Stabilized Pavements," *Proceedings of the 5th International RILEM Conference*, Limonges, France, May 2004.

American Concrete Institute, *State-of-the-Art Report on Soil Cement*, ACI Materials Journal, Vol. 87, No. 4, July/August 1990, pages 395 to 417.

Clegg Instruction Manual, Lafayette Instrument Company, Lafayette, Indiana, 1993.

GeoGauge™ User Guide: Model H-4140 Soil Stiffness and Modulus Gauge, Humboldt Manufacturing Company, Norridge, Illinois, 2002.

Crane, R. A.; Guthrie, W. S.; Eggett, D. L.; and Hanson. J. R., "Roughness of Flexible Pavements with Cement-Treated Base Layers," *Transportation Research Board 85th Annual Meeting Compendium of Papers*, CD-ROM, Transportation Research Board of the National Academies, Washington, D.C., January 2006.

George, K. P., "Mechanism of Shrinkage Cracking of Soil-Cement Bases," Highway Research Record, No. 442, Highway Research Board, Washington, D.C., 1973, pages 1 to 10.

George, K. P., "Minimizing Cracking in Cement-Treated Materials for Improved Performance," RD123, Portland Cement Association, Skokie, Illinois, 2002.

Goehl, D.; Sebesta, S.; and Scullion, T., "Microcracking Stabilized Bases during Construction to Minimize Shrinkage," Product 0-4502-P4, Texas Transportation Institute, Texas A&M University System, College Station, Texas, August 2006.

Guthrie, W. S.; Young T. B.; Blankenagel, B. J.; and D. A. Cooley, "Early-Age Strength Assessment of Cement-Treated Base Material," *Transportation Research Record: Journal of the Transportation Research Board*, No. 1936, Transportation Research Board of the National Academies, Washington, D.C., 2005, pages 12-19.

Hajek, J., "Predicting Low-Temperature Cracking Frequency of Asphalt Concrete Pavements," Highway Research Record, No. 407, Highway Research Board, Washington, D.C., 1972, pages 39 to 54.

Halsted, G., "Pavements: Performance of Soil-Cement and Cement-Modified Soil for Pavements: Research Synopsis," IS691, Portland Cement Association, Skokie, Illinois, 2006.

Hope, C. A.; Wilson, B. T.; and Guthrie, W. S., "Comparison of Dry and Slurry Application Techniques for Cement Stabilization of Aggregate Base Materials," *Transportation Research Board 90th Annual Meeting Compendium of Papers*, CD-ROM, Transportation Research Board of the National Academies, Washington, D.C., January, 2011.

Litzka, J. and Haslehner, W., "Cold In-Place Recycling on Low Volume Roads in Austria," *Proceedings of the Sixth International Conference on Low Volume Roads*, Minneapolis, Minnesota, June 1995.

Luhr, R.; Adaska, W. S.; and Halsted, G. E., "Guide to Full-Depth Reclamation (FDR) with Cement," EB234.01, Portland Cement Association, Skokie, Illinois, 2005.

Mindess, S.; Young, J. F.; and Darwin D., *Concrete*, Second Edition, Prentice Hall, Upper Saddle River, New Jersey, 2003.

Norling, L., "Minimizing Reflective Cracks in Soil-Cement Pavements: A Status Report of Laboratory Studies and Field Practices," Highway Research Record, No. 442, Highway Research Board, Washington, D.C., 1973, pages 22 to 33.

Portland Cement Association, *Soil-Cement Information: Cement-Treated Aggregate Base*, SR221S, Portland Cement Association, Skokie, Illinois, 2006.

Portland Cement Association, *Soil-Cement Information: Reflective Cracking in Cement Stabilized Pavements*, IS537, Portland Cement Association, Skokie, Illinois, 2003.

Pretorius, P.C.; Bruinette; Kruger; Stoffberg; Hugo; and Monismith, C. L., "Fatigue Crack Formation and Propagation in Pavements Containing Soil-Cement Bases," Highway Research Record, No. 407, Highway Research Board, Washington, D.C., 1972, pages 102 to 115.

Prusinski, J. R., "Recycling Flexible Pavements with Cement: Diverse Methods Produce Durable Pavements," Soil-Cement and Other Construction Practices in Geotechnical Engineering, *Proceedings of Sessions of Geo-Denver 2000*, American Society of Civil Engineers, Denver, Colorado, August 5-8, 2000.

Scullion, T., "Field Investigation: Precracking of Soil-Cement Bases to Reduce Reflection Cracking," *Transportation Research Record: Journal of the Transportation Research Board*, No. 1787, Transportation Research Board of the National Academies, Washington, D.C., 2002, pages 22 to 30.

Scullion, T.; Sebesta, S.; Harris, J.P.; and Syed, I., "Evaluating the Performance of Soil-Cement and Cement-Modified Soil for Pavements: A Laboratory Investigation," RD120, Portland Cement Association, Skokie, Illinois, 2005.

Sebesta, S. and Scullion, T., "Effectiveness of Minimizing Reflective Cracking in Cement-Treated Bases by Microcracking," Report 0-4502-1, Texas Transportation Institute, Texas A&M University System, College Station, Texas, 2004.

Sebesta, S., "Continued Evaluation of Microcracking in Texas," Report 0-4502-2, Texas Transportation Institute, Texas A&M University System, College Station, Texas, 2005a.

Sebesta, S., "Microcracking for Reduced Shrinkage in Cement-Treated Base," Report 0-4502-S, Texas Transportation Institute, Texas A&M University System, College Station, Texas, 2006.

Sebesta, S., "Use of Microcracking to Reduce Shrinkage Cracking in Cement Treated Bases," *Transportation Research Board 84th Annual Meeting Compendium of Papers*, CD-ROM, Transportation Research Board of the National Academies, Washington, D.C., January, 2005b.

Thompson, W. M. and Guthrie, W. S., "Correlating Responses of Portable Field Instruments Used for Testing Soil and Aggregate Pavement Layers," *Transportation Research Board 88th Annual Meeting Compendium of Papers*, CD-ROM, Transportation Research Board of the National Academies, Washington, D.C., January 2009.

Wang, J., "Use of Additives and Expansive Cements For Shrinkage Crack Control in Soil-Cement: A Review," Highway Research Record, No. 442, Highway Research Board, Washington, D.C., 1973, pages 11 to 21.

Webster, S. L.; Grau, R. H.; and Williams, R. P, "Description and application of Dual Mass Dynamic Cone Penetrometer," Report GL-92-3, Waterways Experiment Station, U.S. Army Corps of Engineers, Vicksburg, Mississippi, 1992.

APPENDIX A STIFFNESS MEASUREMENTS

Table A-1: CIST Measurements at Redwood Drive

Station	CIV						
	Day of construction	Day of microcracking					3 days after microcracking
		0 passes	1 pass	2 passes	3 passes	4 passes	
1	24.7	34.9	42.8	35.5	-	-	36.9
2	23.7	35.1	38.3	34.0	-	-	39.4
3	15.0	27.3	25.8	27.0	-	-	33.6
4	15.6	47.0	37.8	31.7	-	-	28.9
5	23.5	53.4	45.6	44.9	45.1	49.9	41.3
6	23.2	27.2	29.6	29.8	29.2	27.9	39.7
7	27.0	29.4	36.2	32.6	30.5	33.9	40.9
8	30.5	39.3	35.7	32.2	36.6	31.2	66.1
9	22.7	24.4	23.4	25.8	25.2	30.7	26.2
10	20.1	31.8	31.2	34.1	-	-	27.4
Average	22.6	35.0	34.7	32.8	33.3	34.7	38.0
Std. dev.	4.7	9.3	7.1	5.3	7.8	8.7	11.4
CV (%)	20.9	26.6	20.5	16.1	23.3	25.2	29.9

Table A-2: PFWD Measurements at Redwood Drive

Station	Modulus (ksi)						
	Day of construction	Day of microcracking					3 days after microcracking
		0 passes	1 pass	2 passes	3 passes	4 passes	
1	6.7	38.6	16.4	14.5	-	-	20.1
2	7.8	40.6	16.7	14.7	-	-	25.9
3	10.2	34.1	24.8	17.9	-	-	31.9
4	18.0	52.8	37.6	32.4	-	-	55.8
5	37.6	107.2	85.2	83.6	56.7	33.8	32.8
6	8.7	30.8	21.3	18.6	20.2	18.5	27.8
7	19.3	58.1	44.6	38.0	28.7	32.4	38.0
8	11.0	89.5	48.1	-	24.3	29.6	39.7
9	6.8	22.0	15.1	-	13.0	11.3	16.2
10	14.7	37.3	17.8	25.1	-	-	23.0
Average	14.1	51.1	32.8	30.6	28.6	25.1	31.1
Std. dev.	9.4	27.3	22.1	23.0	16.8	9.8	11.5
CV (%)	66.8	53.3	67.6	75.3	58.7	39.0	36.8

Table A-3: SSG Measurements at Redwood Drive

Station	Stiffness (MN/m)						
	Day of construction	Day of microcracking					3 days after microcracking
		0 passes	1 pass	2 passes	3 passes	4 passes	
1	18.0	47.8	28.5	22.8	-	-	26.6
2	22.8	44.3	24.3	16.2	-	-	32.8
3	17.9	38.3	35.1	24.2	-	-	37.2
4	15.8	51.1	22.3	17.1	-	-	25.2
5	23.8	44.6	48.6	28.5	29.8	20.4	31.7
6	12.8	34.0	24.7	22.8	28.0	18.9	26.6
7	18.8	48.4	27.4	27.2	26.3	16.3	31.6
8	21.6	46.6	26.8	29.7	26.8	20.9	38.5
9	18.4	43.0	22.2	23.6	24.5	19.6	27.2
10	29.1	36.4	22.2	23.8	-	-	24.6
Average	19.9	43.4	28.2	23.6	27.1	19.2	30.2
Std. dev.	4.6	5.6	8.2	4.4	2.0	1.8	4.9
CV (%)	23.0	12.9	28.9	18.5	7.4	9.4	16.4

Table A-4: CIST Measurements at Dale Avenue

Station	CIV			
	Day of construction	Day of microcracking		
		0 passes	1 pass	2 passes
1	14.3	27.7	28.2	27.0
2	19.5	36.5	32.1	27.8
3	19.8	27.4	32.5	30.8
4	-	37.4	32.1	32.0
5	21.7	32.1	29.9	34.5
6	23.4	33.3	38.4	34.5
7	20.8	32.6	43.4	-
8	16.9	29.4	26.9	-
9	23.7	55.7	45.8	-
10	20.3	40.5	38.5	-
Average	20.0	35.2	34.8	31.1
Std. dev.	3.0	8.3	6.4	3.2
CV (%)	14.9	23.7	18.5	10.2

Table A-5: PFWD Measurements at Dale Avenue

Station	Modulus (ksi)			
	Day of construction	Day of microcracking		
		0 passes	1 pass	2 passes
1	10.8	21.5	14.1	13.3
2	19.5	37.9	22.3	22.5
3	10.1	28.4	17.5	13.0
4	10.0	26.3	17.6	14.5
5	13.5	27.2	15.8	14.6
6	16.8	44.6	25.8	25.5
7	7.7	27.0	12.7	-
8	8.6	44.2	16.7	-
9	16.5	108.9	36.7	-
10	9.6	67.0	32.8	-
Average	12.3	43.3	21.2	17.2
Std. dev.	4.0	26.7	8.1	5.4
CV (%)	32.8	61.6	38.4	31.1

Table A-6: SSG Measurements at Dale Avenue

Station	Stiffness (MN/m)			
	Day of construction	Day of microcracking		
		0 passes	1 pass	2 passes
1	14.3	28.1	20.6	21.8
2	19.5	33.6	30.4	22.5
3	19.8	32.2	23.5	21.2
4	17.3	32.4	25.5	19.6
5	20.6	26.1	17.5	16.5
6	23.4	36.8	23.0	25.5
7	20.8	25.3	23.5	-
8	16.9	31.8	26.8	-
9	23.7	32.4	26.2	-
10	20.3	34.1	27.0	-
Average	19.6	31.3	24.4	21.2
Std. dev.	2.9	3.6	3.6	3.0
CV (%)	14.6	11.7	14.8	14.1

Table A-7: CIST Measurements at Spanish Fork

Station	CIV						
	Day of construction	Day of microcracking					3 days after microcracking
		0 passes	1 pass	2 passes	3 passes	4 passes	
1	15.5	22.4	-	-	-	29.7	-
2	13.6	37.8	-	-	-	41.2	-
3	25.4	34.0	-	-	-	38.3	-
4	27.0	28.4	-	-	-	37.5	-
5	17.8	28.6	-	-	-	25.8	-
6	13.4	25.4	-	-	-	24.1	-
7	20.6	29.0	-	-	-	34.6	-
8	13.1	25.0	-	-	-	37.0	-
9	23.0	36.0	-	-	-	38.9	-
10	15.9	31.8	-	-	-	32.8	-
Average	18.5	29.8	-	-	-	34.0	-
Std. dev.	5.2	5.0	-	-	-	5.8	-
CV (%)	28.0	16.8	-	-	-	17.0	-

Table A-8: PFWD Measurements at Spanish Fork

Station	Modulus (ksi)						
	Day of construction	Day of microcracking					3 days after microcracking
		0 passes	1 pass	2 passes	3 passes	4 passes	
1	16.0	47.0	-	-	-	27.9	-
2	21.2	92.8	-	-	-	51.6	-
3	17.2	68.2	-	-	-	49.6	-
4	20.6	45.6	-	-	-	24.0	-
5	14.1	68.2	-	-	-	38.1	-
6	14.7	73.4	-	-	-	32.8	-
7	15.1	41.3	-	-	-	20.2	-
8	13.8	26.0	-	-	-	20.7	-
9	18.4	41.8	-	-	-	26.5	-
10	14.0	53.0	-	-	-	31.3	-
Average	16.5	55.7	-	-	-	32.3	-
Std. dev.	2.8	19.6	-	-	-	11.1	-
CV (%)	16.7	35.2	-	-	-	34.5	-

Table A-9: SSG Measurements at Spanish Fork

Station	Stiffness (MN/m)						
	Day of construction	Day of microcracking					3 days after microcracking
		0 passes	1 pass	2 passes	3 passes	4 passes	
1	9.8	20.7	-	-	-	12.7	-
2	24.7	39.7	-	-	-	31.6	-
3	32.7	42.1	-	-	-	25.2	-
4	27.8	28.4	-	-	-	21.2	-
5	25.5	40.7	-	-	-	24.0	-
6	17.5	21.0	-	-	-	22.0	-
7	20.3	26.2	-	-	-	20.5	-
8	15.9	26.3	-	-	-	13.5	-
9	13.9	30.9	-	-	-	23.7	-
10	21.7	34.2	-	-	-	22.4	-
Average	21.0	31.0	-	-	-	21.7	-
Std. dev.	6.9	7.9	-	-	-	5.5	-
CV (%)	33.0	25.5	-	-	-	25.3	-

Table A-10: CIST Measurements at Wyoming A

Station	CIV						
	Day of construction	Day of microcracking					3 days after microcracking
		0 passes	1 pass	2 passes	3 passes	4 passes	
1	-	36.9	12.3	12.7	-	13.7	-
2	-	47.2	23.8	24.0	-	17.7	-
3	-	40.3	13.8	17.3	-	13.8	-
4	-	40.3	18.7	17.3	-	13.8	-
5	-	40.0	35.1	20.3	-	15.5	-
6	-	47.2	22.4	30.3	-	16.1	-
7	-	46.0	22.9	26.0	-	18.4	-
8	-	24.9	16.0	18.2	-	18.2	-
9	-	15.7	15.0	20.1	-	17.2	-
10	-	22.1	17.0	17.3	-	35.5	-
Average	-	36.1	19.7	20.4	-	18.0	-
Std. dev.	-	11.2	6.7	5.1	-	6.4	-
CV (%)	-	31.1	34.1	25.1	-	35.7	-

Table A-11: PFWD Measurements at Wyoming A

Station	Modulus (ksi)						
	Day of construction	Day of microcracking					3 days after microcracking
		0 passes	1 pass	2 passes	3 passes	4 passes	
1	-	21.4	19.2	17.2	-	17.6	22.0
2	-	35.1	25.1	27.3	-	25.6	28.9
3	-	30.7	24.3	23.6	-	21.5	30.7
4	-	42.7	28.9	29.2	-	26.3	33.5
5	-	41.3	30.8	31.2	-	28.6	35.2
6	-	49.1	40.8	39.1	-	34.3	42.4
7	-	84.9	61.6	60.4	-	59.8	71.2
8	-	47.0	41.1	41.8	-	39.9	41.4
9	-	54.0	49.5	44.1	-	44.8	45.7
10	-	37.1	30.4	30.5	-	26.9	31.7
Average	-	44.3	35.2	34.4	-	32.5	38.3
Std. dev.	-	17.1	13.0	12.3	-	12.6	13.5
CV (%)	-	38.6	37.0	35.7	-	38.8	35.4

Table A-12: SSG Measurements at Wyoming A

Station	Stiffness (MN/m)						
	Day of construction	Day of microcracking					3 days after microcracking
		0 passes	1 pass	2 passes	3 passes	4 passes	
1	-	-	-	-	-	-	-
2	-	-	-	-	-	-	-
3	-	-	-	-	-	-	-
4	-	-	-	-	-	-	-
5	-	-	-	-	-	-	-
6	-	-	-	-	-	-	-
7	-	-	-	-	-	-	-
8	-	-	-	-	-	-	-
9	-	-	-	-	-	-	-
10	-	-	-	-	-	-	-
Average	-	-	-	-	-	-	-
Std. dev.	-	-	-	-	-	-	-
CV (%)	-	-	-	-	-	-	-

Table A-13: CIST Measurements at Wyoming B

Station	CIV						
	Day of construction	Day of microcracking					3 days after microcracking
		0 passes	1 pass	2 passes	3 passes	4 passes	
1	-	17.7	-	-	-	14.8	-
2	-	17.1	-	-	-	13.5	-
3	-	15.2	-	-	-	12.3	-
4	-	24.3	-	-	-	15.1	-
5	-	27.4	-	-	-	22.2	-
6	-	36.9	-	-	-	18.3	-
7	-	14.4	-	-	-	21.2	-
8	-	13.6	-	-	-	15.1	-
9	-	13.6	-	-	-	10.2	-
10	-	37.4	-	-	-	22.4	-
Average	-	21.8	-	-	-	16.5	-
Std. dev.	-	9.3	-	-	-	4.3	-
CV (%)	-	42.8	-	-	-	26.0	-

Table A-14: PFWD Measurements at Wyoming B

Station	Modulus (ksi)						
	Day of construction	Day of microcracking					3 days after microcracking
		0 passes	1 pass	2 passes	3 passes	4 passes	
1	-	24.5	-	-	-	28.7	-
2	-	14.1	-	-	-	13.6	-
3	-	20.0	-	-	-	19.0	-
4	-	78.8	-	-	-	52.7	-
5	-	46.2	-	-	-	44.8	-
6	-	35.0	-	-	-	25.6	-
7	-	44.7	-	-	-	27.5	-
8	-	27.3	-	-	-	21.8	-
9	-	20.6	-	-	-	14.2	-
10	-	51.0	-	-	-	40.7	-
Average	-	36.2	-	-	-	28.9	-
Std. dev.	-	19.5	-	-	-	13.2	-
CV (%)	-	53.8	-	-	-	45.8	-

Table A-15: SSG Measurements at Wyoming B

Station	Stiffness (MN/m)						
	Day of construction	Day of microcracking					3 days after microcracking
		0 passes	1 pass	2 passes	3 passes	4 passes	
1	-	-	-	-	-	-	-
2	-	-	-	-	-	-	-
3	-	-	-	-	-	-	-
4	-	-	-	-	-	-	-
5	-	-	-	-	-	-	-
6	-	-	-	-	-	-	-
7	-	-	-	-	-	-	-
8	-	-	-	-	-	-	-
9	-	-	-	-	-	-	-
10	-	-	-	-	-	-	-
Average	-	-	-	-	-	-	-
Std. dev.	-	-	-	-	-	-	-
CV (%)	-	-	-	-	-	-	-

Table A-16: CIST Measurements at Wyoming C

Station	CIV						
	Day of construction	Day of microcracking					3 days after microcracking
		0 passes	1 pass	2 passes	3 passes	4 passes	
1	-	-	-	-	-	-	-
2	-	-	-	-	-	-	-
3	-	-	-	-	-	-	-
4	-	-	-	-	-	-	-
5	-	-	-	-	-	-	-
6	-	-	-	-	-	-	-
7	-	-	-	-	-	-	-
8	-	-	-	-	-	-	-
9	-	-	-	-	-	-	-
10	-	-	-	-	-	-	-
Average	-	-	-	-	-	-	-
Std. dev.	-	-	-	-	-	-	-
CV (%)	-	-	-	-	-	-	-

Table A-17: PFWD Measurements at Wyoming C

Station	Modulus (ksi)						
	Day of construction	Day of microcracking					3 days after microcracking
		0 passes	1 pass	2 passes	3 passes	4 passes	
1	-	60.5	-	-	-	45.7	-
2	-	13.8	-	-	-	14.4	-
3	-	28.6	-	-	-	23.2	-
4	-	94.8	-	-	-	71.3	-
5	-	31.9	-	-	-	27.2	-
6	-	50.0	-	-	-	44.0	-
7	-	46.1	-	-	-	33.6	-
8	-	46.0	-	-	-	43.7	-
9	-	40.8	-	-	-	39.0	-
10	-	38.8	-	-	-	34.8	-
Average	-	45.1	-	-	-	37.7	-
Std. dev.	-	21.6	-	-	-	15.5	-
CV (%)	-	48.0	-	-	-	41.1	-

Table A-18: SSG Measurements at Wyoming C

Station	Stiffness (MN/m)						
	Day of construction	Day of microcracking					3 days after microcracking
		0 passes	1 pass	2 passes	3 passes	4 passes	
1	-	43.6	-	-	-	28.9	-
2	-	39.9	-	-	-	29.1	-
3	-	37.3	-	-	-	35.3	-
4	-	36.9	-	-	-	34.6	-
5	-	37.8	-	-	-	30.1	-
6	-	36.0	-	-	-	30.6	-
7	-	36.0	-	-	-	30.6	-
8	-	30.9	-	-	-	27.9	-
9	-	25.9	-	-	-	26.0	-
10	-	25.3	-	-	-	22.9	-
Average	-	35.0	-	-	-	29.6	-
Std. dev.	-	5.9	-	-	-	3.7	-
CV (%)	-	16.8	-	-	-	12.4	-

Table A-19: CIST Measurements at Wyoming D

Station	CIV						
	Day of construction	Day of microcracking					3 days after microcracking
		0 passes	1 pass	2 passes	3 passes	4 passes	
1	-	-	-	-	-	-	-
2	-	-	-	-	-	-	-
3	-	-	-	-	-	-	-
4	-	-	-	-	-	-	-
5	-	-	-	-	-	-	-
6	-	-	-	-	-	-	-
7	-	-	-	-	-	-	-
8	-	-	-	-	-	-	-
9	-	-	-	-	-	-	-
10	-	-	-	-	-	-	-
Average	-	-	-	-	-	-	-
Std. dev.	-	-	-	-	-	-	-
CV (%)	-	-	-	-	-	-	-

Table A-20: PFWD Measurements at Wyoming D

Station	Modulus (ksi)						
	Day of construction	Day of microcracking					3 days after microcracking
		0 passes	1 pass	2 passes	3 passes	4 passes	
1	-	32.7	-	-	-	26.9	-
2	-	47.7	-	-	-	30.8	-
3	-	19.5	-	-	-	16.6	-
4	-	39.2	-	-	-	26.9	-
5	-	34.9	-	-	-	28.5	-
6	-	41.4	-	-	-	30.9	-
7	-	63.4	-	-	-	39.9	-
8	-	24.1	-	-	-	19.8	-
9	-	48.7	-	-	-	34.5	-
10	-	45.0	-	-	-	30.8	-
Average	-	39.7	-	-	-	28.6	-
Std. dev.	-	12.7	-	-	-	6.7	-
CV (%)	-	32.1	-	-	-	23.5	-

Table A-21: SSG Measurements at Wyoming D

Station	Stiffness (MN/m)						
	Day of construction	Day of microcracking					3 days after microcracking
		0 passes	1 pass	2 passes	3 passes	4 passes	
1	-	28.3	-	-	-	21.9	-
2	-	37.5	-	-	-	29.8	-
3	-	28.5	-	-	-	24.3	-
4	-	36.9	-	-	-	28.7	-
5	-	35.7	-	-	-	25.8	-
6	-	30.4	-	-	-	23.7	-
7	-	49.4	-	-	-	36.9	-
8	-	25.8	-	-	-	19.2	-
9	-	38.4	-	-	-	26.4	-
10	-	46.1	-	-	-	36.6	-
Average	-	35.7	-	-	-	27.3	-
Std. dev.	-	7.7	-	-	-	5.8	-
CV (%)	-	21.7	-	-	-	21.4	-

Table A-22: CIST Measurements at Wyoming E

Station	CIV						
	Day of construction	Day of microcracking					3 days after microcracking
		0 passes	1 pass	2 passes	3 passes	4 passes	
1	-	-	-	-	-	-	-
2	-	-	-	-	-	-	-
3	-	-	-	-	-	-	-
4	-	-	-	-	-	-	-
5	-	-	-	-	-	-	-
6	-	-	-	-	-	-	-
7	-	-	-	-	-	-	-
8	-	-	-	-	-	-	-
9	-	-	-	-	-	-	-
10	-	-	-	-	-	-	-
Average	-	-	-	-	-	-	-
Std. dev.	-	-	-	-	-	-	-
CV (%)	-	-	-	-	-	-	-

Table A-23: PFWD Measurements at Wyoming E

Station	Modulus (ksi)						
	Day of construction	Day of microcracking					3 days after microcracking
		0 passes	1 pass	2 passes	3 passes	4 passes	
1	-	42.9	-	-	-	27.9	-
2	-	62.4	-	-	-	54.1	-
3	-	48.9	-	-	-	28.3	-
4	-	59.8	-	-	-	46.5	-
5	-	32.0	-	-	-	21.6	-
6	-	25.3	-	-	-	19.3	-
7	-	46.9	-	-	-	48.5	-
8	-	34.0	-	-	-	33.4	-
9	-	32.6	-	-	-	21.9	-
10	-	41.8	-	-	-	24.2	-
11	-	37.7	27.4	25.1	23.8	24.6	-
Average	-	42.2	27.4	25.1	23.8	31.8	-
Std. dev.	-	11.6	-	-	-	12.2	-
CV (%)	-	27.6	-	-	-	38.3	-

Table A-24: SSG Measurements at Wyoming E

Station	Stiffness (MN/m)						
	Day of construction	Day of microcracking					3 days after microcracking
		0 passes	1 pass	2 passes	3 passes	4 passes	
1	-	46.7	-	-	-	30.4	-
2	-	45.8	-	-	-	34.9	-
3	-	38.9	-	-	-	32.2	-
4	-	50.2	-	-	-	34.8	-
5	-	36.7	-	-	-	23.4	-
6	-	28.1	-	-	-	23.9	-
7	-	48.0	-	-	-	28.6	-
8	-	38.9	-	-	-	30.0	-
9	-	40.4	-	-	-	27.3	-
10	-	39.1	-	-	-	33.9	-
11	-	51.3	44.1	41.7	37.8	38.0	-
Average	-	42.2	44.1	41.7	37.8	30.7	-
Std. dev.	-	6.9	-	-	-	4.7	-
CV (%)	-	16.4	-	-	-	15.2	-

Table A-25: CIST Measurements at Wyoming F

Station	CIV						
	Day of construction	Day of microcracking					3 days after microcracking
		0 passes	1 pass	2 passes	3 passes	4 passes	
1	-	-	-	-	-	-	-
2	-	-	-	-	-	-	-
3	-	-	-	-	-	-	-
4	-	-	-	-	-	-	-
5	-	-	-	-	-	-	-
6	-	-	-	-	-	-	-
7	-	-	-	-	-	-	-
8	-	-	-	-	-	-	-
9	-	-	-	-	-	-	-
10	-	-	-	-	-	-	-
Average	-	-	-	-	-	-	-
Std. dev.	-	-	-	-	-	-	-
CV (%)	-	-	-	-	-	-	-

Table A-26: PFWD Measurements at Wyoming F

Station	Modulus (ksi)						
	Day of construction	Day of microcracking					3 days after microcracking
		0 passes	1 pass	2 passes	3 passes	4 passes	
1	-	22.3	19.0	17.3	17.6	16.5	-
2	-	32.1	-	-	-	25.6	-
3	-	53.8	-	-	-	36.9	-
4	-	94.4	-	-	-	72.9	-
5	-	44.3	-	-	-	30.4	-
6	-	15.6	-	-	-	13.2	-
7	-	23.2	-	-	-	19.1	-
8	-	70.4	-	-	-	46.7	-
9	-	39.6	-	-	-	27.7	-
10	-	60.6	-	-	-	53.4	-
11	-	39.7	25.3	19.3	22.4	21.9	-
Average	-	45.1	22.2	18.3	20.0	33.1	-
Std. dev.	-	23.4	4.5	1.4	3.4	18.1	-
CV (%)	-	51.9	20.1	7.7	17.0	54.7	-

Table A-27: SSG Measurements at Wyoming F

Station	Stiffness (MN/m)						
	Day of construction	Day of microcracking					3 days after microcracking
		0 passes	1 pass	2 passes	3 passes	4 passes	
1	-	26.8	22.5	19.2	20.6	18.0	-
2	-	27.1	-	-	-	22.4	-
3	-	41.2	-	-	-	34.8	-
4	-	38.4	-	-	-	31.7	-
5	-	44.2	-	-	-	36.3	-
6	-	32.1	-	-	-	28.7	-
7	-	31.2	-	-	-	24.3	-
8	-	44.3	-	-	-	30.3	-
9	-	31.9	-	-	-	24.6	-
10	-	41.1	-	-	-	28.9	-
11	-	47.0	35.0	30.8	29.7	29.4	-
Average	-	36.8	28.8	25.0	25.2	28.1	-
Std. dev.	-	7.3	8.8	8.2	6.4	5.4	-
CV (%)	-	19.7	30.7	32.8	25.6	19.3	-

APPENDIX B PERCENT CHANGE

Table B-1: Percent Change in CIST Measurements at Redwood Drive

Station	Change in CIV (%)					
	Day of microcracking					3 days after micro-cracking
	0 passes	1 pass	2 passes	3 passes	4 passes	
1	0.0	22.8	1.7	-	-	5.9
2	0.0	8.9	-3.3	-	-	12.2
3	0.0	-5.3	-1.0	-	-	23.1
4	0.0	-19.6	-32.6	-	-	-38.5
5	0.0	-14.5	-15.8	-15.4	-6.6	-22.7
6	0.0	8.9	9.6	7.4	2.6	46.0
7	0.0	23.1	11.0	3.6	15.2	39.2
8	0.0	-9.2	-18.0	-6.8	-20.6	68.1
9	0.0	-3.8	5.9	3.6	25.9	7.7
10	0.0	-1.9	7.2	-	-	-13.7
Average	0.0	1.0	-3.5	-1.5	3.3	12.7
Std. dev.	0.0	14.6	14.2	9.4	18.2	32.7
CV (%)	-	1516.6	-403.7	-611.2	552.0	256.9

Table B-2: Percent Change in PFWD Measurements at Redwood Drive

Station	Change in modulus (%)					
	Day of microcracking					3 days after micro-cracking
	0 passes	1 pass	2 passes	3 passes	4 passes	
1	0.0	-57.5	-62.5	-	-	-48.0
2	0.0	-58.9	-63.8	-	-	-36.1
3	0.0	-27.2	-47.6	-	-	-6.5
4	0.0	-28.8	-38.7	-	-	5.7
5	0.0	-20.5	-22.0	-47.1	-68.4	-69.4
6	0.0	-31.0	-39.6	-34.6	-39.9	-9.7
7	0.0	-23.2	-34.7	-50.6	-44.3	-34.6
8	0.0	-46.2	-	-72.9	-66.9	-55.6
9	0.0	-31.5	-	-40.9	-48.8	-26.4
10	0.0	-52.2	-32.6	-	-	-38.3
Average	0.0	-37.7	-42.7	-49.2	-53.7	-31.9
Std. dev.	0.0	14.5	14.6	14.6	13.2	23.3
CV (%)	-	-38.6	-34.1	-29.6	-24.6	-73.0

Table B-3: Percent Change in SSG Measurements at Redwood Drive

Station	Change in stiffness (%)					
	Day of microcracking					3 days after micro-cracking
	0 passes	1 pass	2 passes	3 passes	4 passes	
1	0.0	-40.4	-52.4	-	-	-44.3
2	0.0	-45.5	-63.5	-	-	-26.5
3	0.0	-18.4	-43.8	-	-	-13.5
4	0.0	-39.4	-53.4	-	-	-31.6
5	0.0	1.0	-40.7	-38.0	-57.7	-34.0
6	0.0	-10.2	-17.0	1.9	-31.3	-3.3
7	0.0	-13.7	-14.2	-17.2	-48.7	-0.4
8	0.0	-24.0	-15.8	-24.1	-40.9	9.0
9	0.0	-19.2	-14.3	-11.1	-28.7	-1.0
10	0.0	-42.7	-38.5	-	-	-36.4
Average	0.0	-25.2	-35.4	-17.7	-41.4	-18.2
Std. dev.	0.0	15.9	18.6	14.8	12.0	18.6
CV (%)	-	-63.0	-52.7	-83.7	-29.1	-102.3

Table B-4: Percent Change in CIST Measurements at Dale Avenue

Station	Change in CIV (%)		
	Day of microcracking		
	0 passes	1 pass	2 passes
1	0.0	2.0	-2.3
2	0.0	-12.1	-23.7
3	0.0	18.6	12.3
4	0.0	-14.2	-14.4
5	0.0	-6.9	7.5
6	0.0	15.3	3.6
7	0.0	33.4	-
8	0.0	-8.4	-
9	0.0	-17.7	-
10	0.0	-4.9	-
Average	0.0	0.5	-2.8
Std. dev.	0.0	16.7	13.8
CV (%)	-	3178.6	-484.7

Table B-5: Percent Change in PFWD Measurements at Dale Avenue

Station	Change in modulus (%)		
	Day of microcracking		
	0 passes	1 pass	2 passes
1	0.0	-34.4	-38.2
2	0.0	-41.1	-40.7
3	0.0	-38.5	-54.4
4	0.0	-33.2	-45.1
5	0.0	-42.1	-46.3
6	0.0	-42.2	-42.8
7	0.0	-53.1	-
8	0.0	-62.1	-
9	0.0	-66.3	-
10	0.0	-51.0	-
Average	0.0	-46.4	-44.6
Std. dev.	0.0	11.3	5.6
CV (%)	-	-24.4	-12.6

Table B-6: Percent Change in SSG Measurements at Dale Avenue

Station	Change in stiffness (%)		
	Day of microcracking		
	0 passes	1 pass	2 passes
1	0.0	-26.8	-22.4
2	0.0	-9.5	-33.0
3	0.0	-27.0	-34.2
4	0.0	-21.2	-39.5
5	0.0	-32.8	-36.7
6	0.0	-37.4	-30.7
7	0.0	-7.0	-
8	0.0	-15.7	-
9	0.0	-19.1	-
10	0.0	-20.6	-
Average	0.0	-21.7	-32.7
Std. dev.	0.0	9.6	5.9
CV (%)	-	-44.3	-18.1

Table B-7: Percent Change in CIST Measurements at Spanish Fork

Station	Change in CIV (%)					
	Day of microcracking					3 days after micro-cracking
	0 passes	1 pass	2 passes	3 passes	4 passes	
1	0.0	-	-	-	32.9	-
2	0.0	-	-	-	9.2	-
3	0.0	-	-	-	12.6	-
4	0.0	-	-	-	32.0	-
5	0.0	-	-	-	-9.6	-
6	0.0	-	-	-	-5.2	-
7	0.0	-	-	-	19.3	-
8	0.0	-	-	-	47.9	-
9	0.0	-	-	-	7.9	-
10	0.0	-	-	-	3.4	-
Average	0.0	-	-	-	15.0	-
Std. dev.	0.0	-	-	-	18.1	-
CV (%)	-	-	-	-	120.4	-

Table B-8: Percent Change in PFWD Measurements at Spanish Fork

Station	Change in modulus (%)					
	Day of microcracking					3 days after micro-cracking
	0 passes	1 pass	2 passes	3 passes	4 passes	
1	0.0	-	-	-	-40.6	-
2	0.0	-	-	-	-44.4	-
3	0.0	-	-	-	-27.2	-
4	0.0	-	-	-	-47.4	-
5	0.0	-	-	-	-44.2	-
6	0.0	-	-	-	-55.3	-
7	0.0	-	-	-	-51.1	-
8	0.0	-	-	-	-20.5	-
9	0.0	-	-	-	-36.6	-
10	0.0	-	-	-	-41.0	-
Average	0.0	-	-	-	-40.8	-
Std. dev.	0.0	-	-	-	10.5	-
CV (%)	-	-	-	-	-25.8	-

Table B-9: Percent Change in SSG Measurements at Spanish Fork

Station	Change in stiffness (%)					
	Day of microcracking					3 days after micro-cracking
	0 passes	1 pass	2 passes	3 passes	4 passes	
1	0.0	-	-	-	-38.8	-
2	0.0	-	-	-	-20.4	-
3	0.0	-	-	-	-40.0	-
4	0.0	-	-	-	-25.5	-
5	0.0	-	-	-	-41.2	-
6	0.0	-	-	-	4.7	-
7	0.0	-	-	-	-22.0	-
8	0.0	-	-	-	-48.7	-
9	0.0	-	-	-	-23.3	-
10	0.0	-	-	-	-34.5	-
Average	0.0	-	-	-	-29.0	-
Std. dev.	0.0	-	-	-	15.2	-
CV (%)	-	-	-	-	-52.6	-

Table B-10: Percent Change in CIST Measurements at Wyoming A

Station	Change in CIV (%)					
	Day of microcracking					3 days after micro-cracking
	0 passes	1 pass	2 passes	3 passes	4 passes	
1	0.0	-66.7	-65.6	-	-62.9	-
2	0.0	-49.6	-49.2	-	-62.5	-
3	0.0	-65.8	-57.1	-	-65.8	-
4	0.0	-53.6	-57.1	-	-65.8	-
5	0.0	-12.3	-49.3	-	-61.3	-
6	0.0	-52.5	-35.8	-	-65.9	-
7	0.0	-50.2	-43.5	-	-60.0	-
8	0.0	-35.7	-26.9	-	-26.9	-
9	0.0	-4.5	28.0	-	9.6	-
10	0.0	-23.1	-21.7	-	60.6	-
Average	0.0	-41.4	-37.8	-	-40.1	-
Std. dev.	0.0	21.7	26.9	-	43.0	-
CV (%)	-	-52.4	-71.2	-	-107.3	-

Table B-11: Percent Change in PFWD Measurements at Wyoming A

Station	Change in modulus (%)					
	Day of microcracking					3 days after micro-cracking
	0 passes	1 pass	2 passes	3 passes	4 passes	
1	0.0	-10.3	-19.6	-	-17.8	2.8
2	0.0	-28.5	-22.2	-	-27.1	-17.7
3	0.0	-20.8	-23.1	-	-30.0	0.0
4	0.0	-32.3	-31.6	-	-38.4	-21.5
5	0.0	-25.4	-24.5	-	-30.8	-14.8
6	0.0	-16.9	-20.4	-	-30.1	-13.6
7	0.0	-27.4	-28.9	-	-29.6	-16.1
8	0.0	-12.6	-11.1	-	-15.1	-11.9
9	0.0	-8.3	-18.3	-	-17.0	-15.4
10	0.0	-18.1	-17.8	-	-27.5	-14.6
Average	0.0	-20.1	-21.7	-	-26.3	-12.3
Std. dev.	0.0	8.2	5.8	-	7.4	7.7
CV (%)	-	-41.0	-26.8	-	-28.1	-62.5

Table B-12: Percent Change in SSG Measurements at Wyoming A

Station	Change in stiffness (%)					
	Day of microcracking					3 days after micro-cracking
	0 passes	1 pass	2 passes	3 passes	4 passes	
1	-	-	-	-	-	-
2	-	-	-	-	-	-
3	-	-	-	-	-	-
4	-	-	-	-	-	-
5	-	-	-	-	-	-
6	-	-	-	-	-	-
7	-	-	-	-	-	-
8	-	-	-	-	-	-
9	-	-	-	-	-	-
10	-	-	-	-	-	-
Average	-	-	-	-	-	-
Std. dev.	-	-	-	-	-	-
CV (%)	-	-	-	-	-	-

Table B-13: Percent Change in CIST Measurements at Wyoming B

Station	Change in CIV (%)					
	Day of microcracking					3 days after micro-cracking
	0 passes	1 pass	2 passes	3 passes	4 passes	
1	0.0	-	-	-	-16.4	-
2	0.0	-	-	-	-21.1	-
3	0.0	-	-	-	-19.1	-
4	0.0	-	-	-	-37.9	-
5	0.0	-	-	-	-19.0	-
6	0.0	-	-	-	-50.4	-
7	0.0	-	-	-	47.2	-
8	0.0	-	-	-	11.0	-
9	0.0	-	-	-	-25.0	-
10	0.0	-	-	-	-40.1	-
Average	0.0	-	-	-	-17.1	-
Std. dev.	0.0	-	-	-	28.1	-
CV (%)	-	-	-	-	-164.4	-

Table B-14: Percent Change in PFWD Measurements at Wyoming B

Station	Change in modulus (%)					
	Day of microcracking					3 days after micro-cracking
	0 passes	1 pass	2 passes	3 passes	4 passes	
1	0.0	-	-	-	17.1	-
2	0.0	-	-	-	-3.5	-
3	0.0	-	-	-	-5.0	-
4	0.0	-	-	-	-33.1	-
5	0.0	-	-	-	-3.0	-
6	0.0	-	-	-	-26.9	-
7	0.0	-	-	-	-38.5	-
8	0.0	-	-	-	-20.1	-
9	0.0	-	-	-	-31.1	-
10	0.0	-	-	-	-20.2	-
Average	0.0	-	-	-	-16.4	-
Std. dev.	0.0	-	-	-	17.4	-
CV (%)	-	-	-	-	-105.8	-

Table B-15: Percent Change in SSG Measurements at Wyoming B

Station	Change in stiffness (%)					
	Day of microcracking					3 days after micro-cracking
	0 passes	1 pass	2 passes	3 passes	4 passes	
1	-	-	-	-	-	-
2	-	-	-	-	-	-
3	-	-	-	-	-	-
4	-	-	-	-	-	-
5	-	-	-	-	-	-
6	-	-	-	-	-	-
7	-	-	-	-	-	-
8	-	-	-	-	-	-
9	-	-	-	-	-	-
10	-	-	-	-	-	-
Average	-	-	-	-	-	-
Std. dev.	-	-	-	-	-	-
CV (%)	-	-	-	-	-	-

Table B-16: Percent Change in CIST Measurements at Wyoming C

Station	Change in CIV (%)					
	Day of microcracking					3 days after micro-cracking
	0 passes	1 pass	2 passes	3 passes	4 passes	
1	-	-	-	-	-	-
2	-	-	-	-	-	-
3	-	-	-	-	-	-
4	-	-	-	-	-	-
5	-	-	-	-	-	-
6	-	-	-	-	-	-
7	-	-	-	-	-	-
8	-	-	-	-	-	-
9	-	-	-	-	-	-
10	-	-	-	-	-	-
Average	-	-	-	-	-	-
Std. dev.	-	-	-	-	-	-
CV (%)	-	-	-	-	-	-

Table B-17: Percent Change in PFWD Measurements at Wyoming C

Station	Change in modulus (%)					
	Day of microcracking					3 days after micro-cracking
	0 passes	1 pass	2 passes	3 passes	4 passes	
1	0.0	-	-	-	-24.5	-
2	0.0	-	-	-	4.3	-
3	0.0	-	-	-	-18.9	-
4	0.0	-	-	-	-24.8	-
5	0.0	-	-	-	-14.7	-
6	0.0	-	-	-	-12.0	-
7	0.0	-	-	-	-27.1	-
8	0.0	-	-	-	-5.0	-
9	0.0	-	-	-	-4.4	-
10	0.0	-	-	-	-10.3	-
Average	0.0	-	-	-	-13.7	-
Std. dev.	0.0	-	-	-	10.3	-
CV (%)	-	-	-	-	-74.7	-

Table B-18: Percent Change in SSG Measurements at Wyoming C

Station	Change in stiffness (%)					
	Day of microcracking					3 days after micro-cracking
	0 passes	1 pass	2 passes	3 passes	4 passes	
1	0.0	-	-	-	-33.9	-
2	0.0	-	-	-	-27.1	-
3	0.0	-	-	-	-5.4	-
4	0.0	-	-	-	-6.2	-
5	0.0	-	-	-	-20.4	-
6	0.0	-	-	-	-15.0	-
7	0.0	-	-	-	-15.0	-
8	0.0	-	-	-	-9.7	-
9	0.0	-	-	-	0.4	-
10	0.0	-	-	-	-9.5	-
Average	0.0	-	-	-	-14.2	-
Std. dev.	0.0	-	-	-	10.5	-
CV (%)	-	-	-	-	-74.0	-

Table B-19: Percent Change in CIST Measurements at Wyoming D

Station	Change in CIV (%)					
	Day of microcracking					3 days after micro-cracking
	0 passes	1 pass	2 passes	3 passes	4 passes	
1	-	-	-	-	-	-
2	-	-	-	-	-	-
3	-	-	-	-	-	-
4	-	-	-	-	-	-
5	-	-	-	-	-	-
6	-	-	-	-	-	-
7	-	-	-	-	-	-
8	-	-	-	-	-	-
9	-	-	-	-	-	-
10	-	-	-	-	-	-
Average	-	-	-	-	-	-
Std. dev.	-	-	-	-	-	-
CV (%)	-	-	-	-	-	-

Table B-20: Percent Change in PFWD Measurements at Wyoming D

Station	Change in modulus (%)					
	Day of microcracking					3 days after micro-cracking
	0 passes	1 pass	2 passes	3 passes	4 passes	
1	0.0	-	-	-	-17.7	-
2	0.0	-	-	-	-35.4	-
3	0.0	-	-	-	-14.9	-
4	0.0	-	-	-	-31.4	-
5	0.0	-	-	-	-18.3	-
6	0.0	-	-	-	-25.4	-
7	0.0	-	-	-	-37.1	-
8	0.0	-	-	-	-17.8	-
9	0.0	-	-	-	-29.2	-
10	0.0	-	-	-	-31.6	-
Average	0.0	-	-	-	-25.9	-
Std. dev.	0.0	-	-	-	8.2	-
CV (%)	-	-	-	-	-31.5	-

Table B-21: Percent Change in SSG Measurements at Wyoming D

Station	Change in stiffness (%)					
	Day of microcracking					3 days after micro-cracking
	0 passes	1 pass	2 passes	3 passes	4 passes	
1	0.0	-	-	-	-22.6	-
2	0.0	-	-	-	-20.5	-
3	0.0	-	-	-	-14.7	-
4	0.0	-	-	-	-22.2	-
5	0.0	-	-	-	-27.7	-
6	0.0	-	-	-	-22.0	-
7	0.0	-	-	-	-25.3	-
8	0.0	-	-	-	-25.6	-
9	0.0	-	-	-	-31.3	-
10	0.0	-	-	-	-20.6	-
Average	0.0	-	-	-	-23.3	-
Std. dev.	0.0	-	-	-	4.5	-
CV (%)	-	-	-	-	-19.4	-

Table B-22: Percent Change in CIST Measurements at Wyoming E

Station	Change in CIV (%)					
	Day of microcracking					3 days after micro-cracking
	0 passes	1 pass	2 passes	3 passes	4 passes	
1	-	-	-	-	-	-
2	-	-	-	-	-	-
3	-	-	-	-	-	-
4	-	-	-	-	-	-
5	-	-	-	-	-	-
6	-	-	-	-	-	-
7	-	-	-	-	-	-
8	-	-	-	-	-	-
9	-	-	-	-	-	-
10	-	-	-	-	-	-
Average	-	-	-	-	-	-
Std. dev.	-	-	-	-	-	-
CV (%)	-	-	-	-	-	-

Table B-23: Percent Change in PFWD Measurements at Wyoming E

Station	Change in modulus (%)					
	Day of microcracking					3 days after micro-cracking
	0 passes	1 pass	2 passes	3 passes	4 passes	
1	0.0	-	-	-	-35.0	-
2	0.0	-	-	-	-13.3	-
3	0.0	-	-	-	-42.1	-
4	0.0	-	-	-	-22.2	-
5	0.0	-	-	-	-32.5	-
6	0.0	-	-	-	-23.7	-
7	0.0	-	-	-	3.4	-
8	0.0	-	-	-	-1.8	-
9	0.0	-	-	-	-32.8	-
10	0.0	-	-	-	-42.1	-
11	0.0	-27.3	-33.4	-36.9	-34.7	-
Average	0.0	-27.3	-33.4	-36.9	-25.2	-
Std. dev.	0.0	-	-	-	15.5	-
CV (%)	-	-	-	-	-61.4	-

Table B-24: Percent Change in SSG Measurements at Wyoming E

Station	Change in stiffness (%)					
	Day of microcracking					3 days after micro-cracking
	0 passes	1 pass	2 passes	3 passes	4 passes	
1	0.0	-	-	-	-34.9	-
2	0.0	-	-	-	-23.8	-
3	0.0	-	-	-	-17.2	-
4	0.0	-	-	-	-30.7	-
5	0.0	-	-	-	-36.2	-
6	0.0	-	-	-	-14.9	-
7	0.0	-	-	-	-40.4	-
8	0.0	-	-	-	-22.9	-
9	0.0	-	-	-	-32.4	-
10	0.0	-	-	-	-13.3	-
11	0.0	-14.0	-18.7	-26.3	-25.9	-
Average	0.0	-14.0	-18.7	-26.3	-26.6	-
Std. dev.	0.0	-	-	-	9.1	-
CV (%)	-	-	-	-	-34.2	-

Table B-25: Percent Change in CIST Measurements at Wyoming F

Station	Change in CIV (%)					
	Day of microcracking					3 days after micro-cracking
	0 passes	1 pass	2 passes	3 passes	4 passes	
1	0.0	-	-	-	-	-
2	0.0	-	-	-	-	-
3	0.0	-	-	-	-	-
4	0.0	-	-	-	-	-
5	0.0	-	-	-	-	-
6	0.0	-	-	-	-	-
7	0.0	-	-	-	-	-
8	0.0	-	-	-	-	-
9	0.0	-	-	-	-	-
10	0.0	-	-	-	-	-
Average	0.0	-	-	-	-	-
Std. dev.	0.0	-	-	-	-	-
CV (%)	-	-	-	-	-	-

Table B-26: Percent Change in PFWD Measurements at Wyoming F

Station	Change in modulus (%)					
	Day of microcracking					3 days after micro-cracking
	0 passes	1 pass	2 passes	3 passes	4 passes	
1	0.0	-14.8	-22.4	-21.1	-26.0	-
2	0.0	-	-	-	-20.2	-
3	0.0	-	-	-	-31.4	-
4	0.0	-	-	-	-22.8	-
5	0.0	-	-	-	-31.4	-
6	0.0	-	-	-	-15.4	-
7	0.0	-	-	-	-17.7	-
8	0.0	-	-	-	-33.7	-
9	0.0	-	-	-	-30.1	-
10	0.0	-	-	-	-11.9	-
11	0.0	-36.3	-51.4	-43.6	-44.8	-
Average	0.0	-25.5	-36.9	-32.3	-25.9	-
Std. dev.	0.0	15.2	20.5	15.9	9.6	-
CV (%)	-	-59.5	-55.5	-49.2	-36.8	-

Table B-27: Percent Change in SSG Measurements at Wyoming F

Station	Change in stiffness (%)					
	Day of microcracking					3 days after micro-cracking
	0 passes	1 pass	2 passes	3 passes	4 passes	
1	0.0	-16.0	-28.4	-23.1	-32.8	-
2	0.0	-	-	-	-17.3	-
3	0.0	-	-	-	-15.5	-
4	0.0	-	-	-	-17.4	-
5	0.0	-	-	-	-17.9	-
6	0.0	-	-	-	-10.6	-
7	0.0	-	-	-	-22.1	-
8	0.0	-	-	-	-31.6	-
9	0.0	-	-	-	-22.9	-
10	0.0	-	-	-	-29.7	-
11	0.0	-25.5	-34.5	-36.8	-37.4	-
Average	0.0	-20.8	-31.4	-30.0	-23.2	-
Std. dev.	0.0	6.7	4.3	9.7	8.5	-
CV (%)	-	-32.3	-13.8	-32.3	-36.6	-